

Development of an On-the-Go Automatic Bit-Changing Mechanism for Robotic Screwdrivers: Design, Material Selection, and Analysis

ABSTRACT: The rise of electric vehicles has increased the demand for efficient disassembly of electric car batteries. Robotic screwdrivers play a critical role in the disassembly process. However, the need for frequent tool changes, due to the variety of screw types and sizes used in battery assemblies, poses a significant challenge to maintaining efficiency. This project aims to design an automatic, on-the-go screw bit changer for robotic screwdrivers, which can be seamlessly integrated with industrial robots. The system also enhances operational safety by reducing human involvement in potentially hazardous environments. The design integrates a chain magazine system, driven by sprockets and a Geneva mechanism. Key components of the system, including the tool arm, swing arm, attachment, and sprockets, were modelled in SolidWorks and structurally validated through Finite Element Analysis (FEA) using SolidWorks Simulation. The FEA results demonstrated that all components operate well within their respective material yield strengths. The study concludes that the design meets reliability standards for industrial applications, with suggestions for further research on reducing the attachment's weight and exploring alternative materials like carbon fiber for critical components to enhance performance.

KEY WORDS: Automated tool changer, Bit changing mechanism, Battery disassembly, Robotic screwdrivers, Finite element analysis

1 INTRODUCTION

The rise of electric vehicles has led to a growing demand for efficient and automated systems for the disassembly of electric car batteries. These batteries, composed of various materials and components, require precise handling and disassembly processes to ensure safety, maximize material recovery, and prepare them for recycling or repurposing. In this context, robotic screwdrivers play a critical role in the disassembly process, performing tasks such as removing screws and separating battery modules with high precision. [1] However, the need for frequent tool changes, due to the variety of screw types and sizes used in battery assemblies, poses a significant challenge to maintaining efficiency.

The primary aim of this project is to design an on-the-go automatic screw bit changer for robotic (pneumatic and electric) screwdrivers that can be seamlessly integrated with industrial robots. The bit changer is intended to accommodate a variety of screw sizes and shapes, with flexibility for future expansion to handle more types of fasteners. Additionally, the design will be validated through structural analysis using finite element (FE) software, ensuring its reliability in real-world industrial applications.

The importance of this project is highlighted by its potential impact on both industrial practices and academic research. From an industrial perspective, the disassembly of electric car batteries is a labour-intensive and time-consuming process, often requiring manual intervention for tool changes. [2] A study by Laura identifies common challenges in battery pack disassembly, such as lack of standardization across manufacturers, which raises the need for frequent tool changes during disassembly of different battery packs. [3] An automatic tool change mechanism integrated into a robotic disassembly cell can dramatically improve efficiency, reduce downtime, and enhance the safety of operations by minimizing human involvement in potentially hazardous environments. This innovation is crucial as the automotive industry seeks to scale up the recycling and reuse of electric car batteries to meet sustainability goals and manage the growing volume of end-of-life batteries. [4]

Academically, this project addresses a significant gap in the existing literature. While much research has been conducted on robotic disassembly processes and the automation of various stages of battery recycling, there is limited focus on the tool change mechanisms necessary to facilitate these processes. Existing studies on automatic tool changers, such as those used in CNC machining and robotic arms, provide valuable insights but do not fully address the unique challenges posed by the disassembly of electric car batteries.

Mustafa conducted research on the design of an automatic tool changer with disc magazine for quick tool changes in CNC machines, emphasizing the importance of speed and precision. [5] A study by Ian McLaren demonstrated the development of a tool changer for a reconfigurable machine tool, utilizing a tool changer that is fixed on the machine base. [6] However, these approaches are either too bulky or not adaptable enough for the requirements of robotic screwdrivers used in battery disassembly.

Wei Hua Chen designed a bit-changing mechanism for the robotic disassembly of battery packs, with the mechanism positioned on the workbench. Instead of using a dedicated screwdriver, the robotic arm itself was rotated to screw and unscrew, which resulted in reduced efficiency compared to using an electric screwdriver. [7]

A study by Alireza presents a method for unscrewing hexagonal nuts of various sizes using a compliant robot with a two-finger gripper. This approach uses surface exploration and tactile perception instead of traditional motorized tools, making it ineffective for unscrewing flat head screws. [8] A research by Feldmann discusses the development of a drill driver tool designed for unscrewing various screw types and sizes. This tool can either use existing working points

or create new ones by drilling, allowing it to unscrew screws like cross recessed, slotted, and hexagon sockets. [9] The unscrewing method described by Seliger involves a flexible tool that generates new acting surfaces on screw heads using a pneumatically driven internal impact mass. [10] The destructive nature of these processes restricts their application to products intended for recycling.

By developing a compact, modular, and efficient tool change mechanism, this project aims to fill this gap, offering a solution that can be directly applied to the robotic disassembly. The design will consider the specific needs of disassembly, such as the variety of screw types, the need for rapid and precise tool changes, and the integration with existing robotic systems in a disassembly cell. By adapting and miniaturizing the principles used in larger CNC tool change systems, this research aims to create a solution that is both effective and practical for smaller-scale applications. The proposed tool change mechanism is designed to be seamlessly integrated into existing robotic screwdriver systems, offering a high level of flexibility and operational efficiency, thereby supporting the automotive industry's shift toward more sustainable practices.

This report is organized to provide a progression from design to evaluation of the automatic screw bit changing mechanism. Following the introduction, the report proceeds with the Methods section, which outlines the design process of the mechanism, including material selection, assembly, and control system integration. After that the structural integrity of the design is evaluated through Finite Element Analysis (FEA). In the Results section, the outcomes of the FEA are presented, demonstrating the performance of key components under operational conditions. Finally, the report concludes with a Discussion and Conclusion, where the findings are analysed, potential improvements are suggested, and future research directions are proposed.

2 METHODS

In this project, a chain magazine-type tool changer integrated with sprockets and a Geneva mechanism to facilitate tool advancements is designed. The entire assembly is mounted directly onto the robotic screwdriver, allowing for seamless tool changes without the need for manual intervention. The following sections detail the design, material selection, assembly, structural analysis and implementation process, including the software and equipment used, to ensure that the methodology can be accurately replicated.

2.1 DESIGN

The design process was carried out using SolidWorks 2024 (Dassault Systèmes, Vélizy-Villacoublay, France). The assembly can be divided into three functional parts. Design of each part is given below

2.1.1 Chain Magazine

The tool magazine was designed as a chain structure with sprockets positioned to facilitate smooth tool advancements. The chain holds multiple tools and can be customized to include more or fewer as needed. The design of the chain is based on ASME B29.4 No. 80 double-pitch conveyor roller chain [11], modified with increased-length links to reduce bulk compared to using higher-number chains. This allows for larger attachments while optimizing the chain for its primary function as a tool holder, rather than a load-bearing component. The chosen chain, with a pitch of 75 mm, is commonly used in conveyor systems within the food processing industry due to its compact and efficient design. [12]

The chain assembly consists of five components: the inner link, attachment link, guide roller, pivot pin, and e-clip washer. The inner link connects to the attachment links to form the continuous chain, while the guide rollers ensure smooth movement along the sprockets. The pivot pin holds the links together, and the retaining washer secures the assembly. Detailed engineering drawings for each of these components can be found in Appendix A, where exact dimensions are provided for manufacturing. Figure 1 gives a visual depiction of the inner and outer links, which together form the foundational framework of the chain drive.

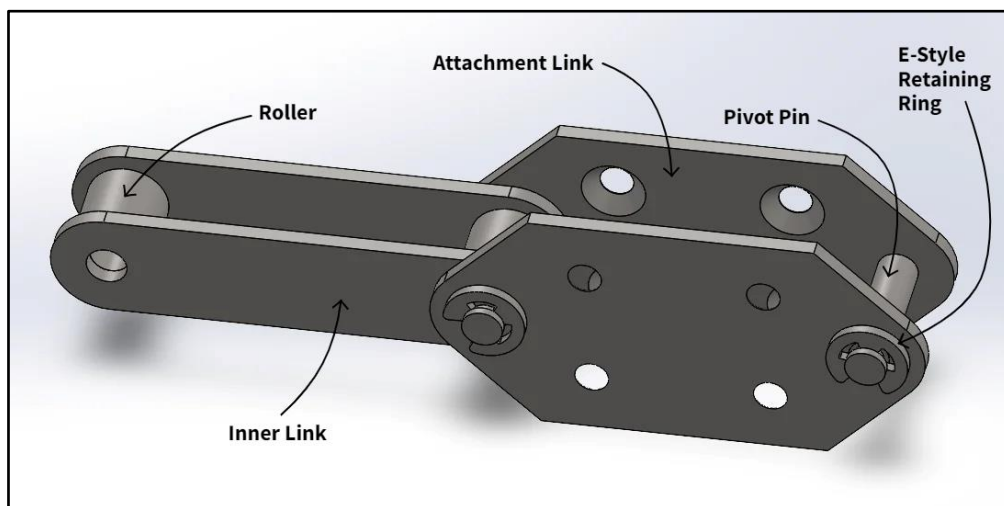


Figure 1: Schematic of assembled chain components

The tool holder assembly is mounted onto the attachment link using four M6 counter sunk machine screws, ensuring a secure connection. Both the attachment and tool arm are machined from aluminium for durability and lightweight properties. The tool arm is connected to the attachment via a self-lubricating brass bushing, which slides onto a stainless dowel pin press-fitted into the attachment, allowing for smooth movement.

The tool arm can be positioned either perpendicular or parallel to chain's plane of motion, achieved by a snap-lock mechanism using spring-loaded ball bearings. These ball bearings are located on either side of the tool arm base and snap into corresponding cavities, ensuring precise positioning and stability in both orientations.

To hold the tools, a needle roller bearing is press-fit into the tool arm, with a 3/8-inch square socket extension inserted into the bearing to allow for smooth, wear-free tool rotation. Detailed engineering drawings of all components, along with exact dimensions for manufacturing, are provided in Appendix A. Figure 2 visually depicts the assembly of tool holding mechanism.

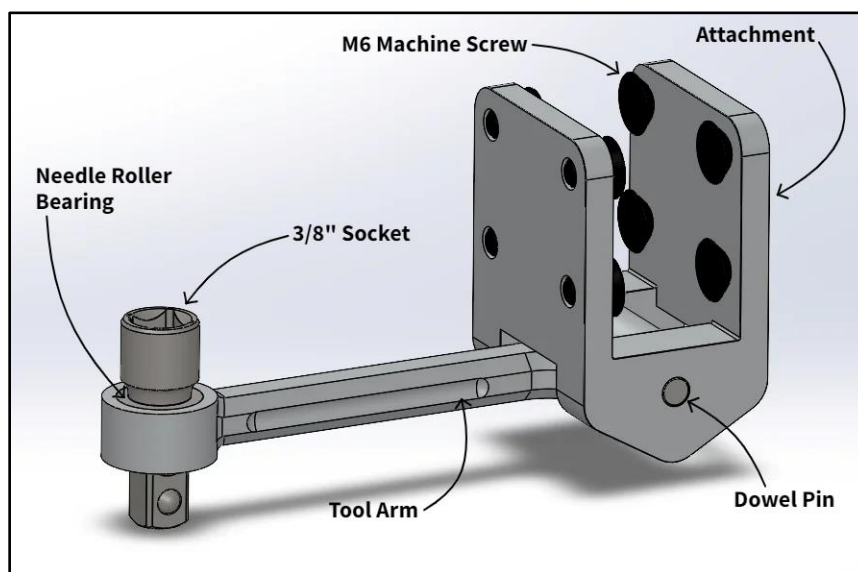


Figure 2: Assembly of attachment

2.1.2 Sprockets and Geneva Mechanism

The sprockets in this design are custom engineered following the ASME B29.1 standard for sprocket design, with specific adaptations to accommodate the modified chain. Due to the increased pitch distance in the chain, a double-pitch single-cut sprocket configuration was selected to ensure compatibility.[11] Typically, the number of teeth on a sprocket is determined by power and speed requirements. [11] However, since this application does not require high power or speed, the number of teeth was flexible and could be chosen freely. To maintain a compact design, the sprocket size was minimized. Given that a polygon must have a minimum of five sides, the sprocket was designed with five teeth, ensuring a balance between small size and functional engagement with the chain. For additional weight reduction, structural modifications like slots are added in non-critical areas. These changes help to reduce weight while maintaining the necessary strength and functionality of the sprocket.

The diameter of the sprocket, also known as the pitch diameter (PD), that circumscribes the pitch polygon is determined using the following formula: [11]

$$PD = \frac{P}{\sin (180/N)}$$

where N represents the number of sides of the polygon, and P is the pitch of the chain. For this design, with a pitch P=75 mm and N=5 sides, the pitch diameter is calculated as:

$$PD = \frac{75 \text{ mm}}{\sin (180/5)} = 127.6 \text{ mm}$$

The distance between the two sprockets i.e. 325 mm, along with other critical dimensions, is determined based on the ASME B29.1 standards. [11] Detailed engineering drawings of the sprocket, including exact dimensions for manufacturing, are available in Appendix A.

For tool advancement, while a stepper motor would be an ideal option, a more cost-effective yet equally efficient alternative, the Geneva mechanism, is chosen. The number of slots in the Geneva wheel matches the number of sprocket teeth, which in this case is five, allowing for one tooth advancement per slot. Since every alternate chain link is used for tool attachment, a drive wheel with two crank pins is required to move the Geneva wheel to the next tool change position with each complete rotation of the drive wheel.

The remaining dimensions of the Geneva mechanism are not critical to this application and were chosen arbitrarily based on design from the Machine Design Databook [13]. For driving the mechanism, a geared DC motor with encoders was selected, as it provides precise control and serves as a more cost-effective alternative to a stepper motor. A visual representation of sprocket coupled with Geneva mechanism is given in Figure 3.

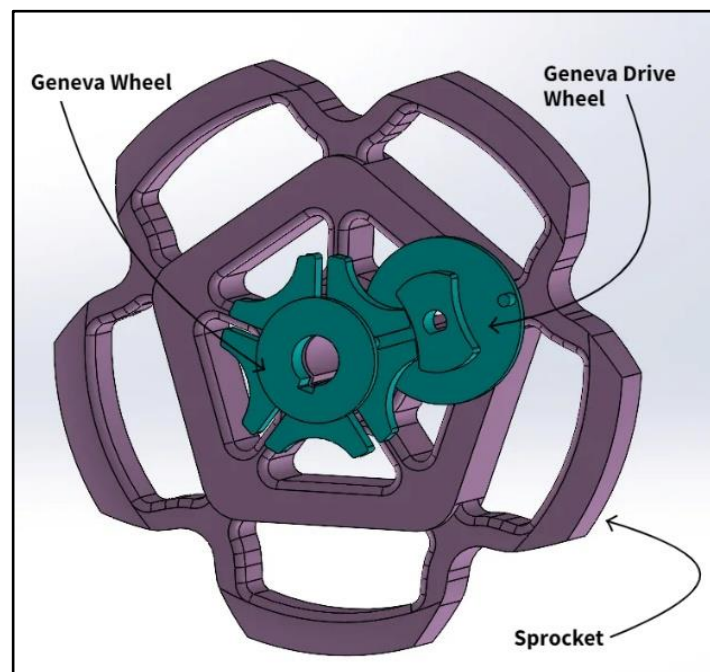


Figure 3: Depiction of sprocket coupled with geneva mechanism

2.1.3 Tool Swing Mechanism

The tool is brought onto the spindle via a swing arm equipped with two spring-loaded ball bearings, which glide along the surface of the tool arm during forward motion. The tool arm moves in a quarter-circle from its advancement position to its snapped-in position. At the end of this travel, the swing arm moves slightly further to ensure the socket is securely attached to the spindle. At this point, the ball bearings snap into designated slots on the sides of the tool arm, locking it in place for reverse rotation and securing the mechanism for screwing or unscrewing operations.

Once the operation is complete, the swing arm rotates in the opposite direction, causing the ball bearings to ride back into the slots, retracting the tool arm. A stop is positioned at the end of the motion to prevent the tool arm from moving too far backward. When this stop is reached, the ball bearings snap out of the slot, making the system ready for the next tool change cycle. The motion of the tool change mechanism is illustrated in Figure 4, showing the transition from tool engagement to retraction.

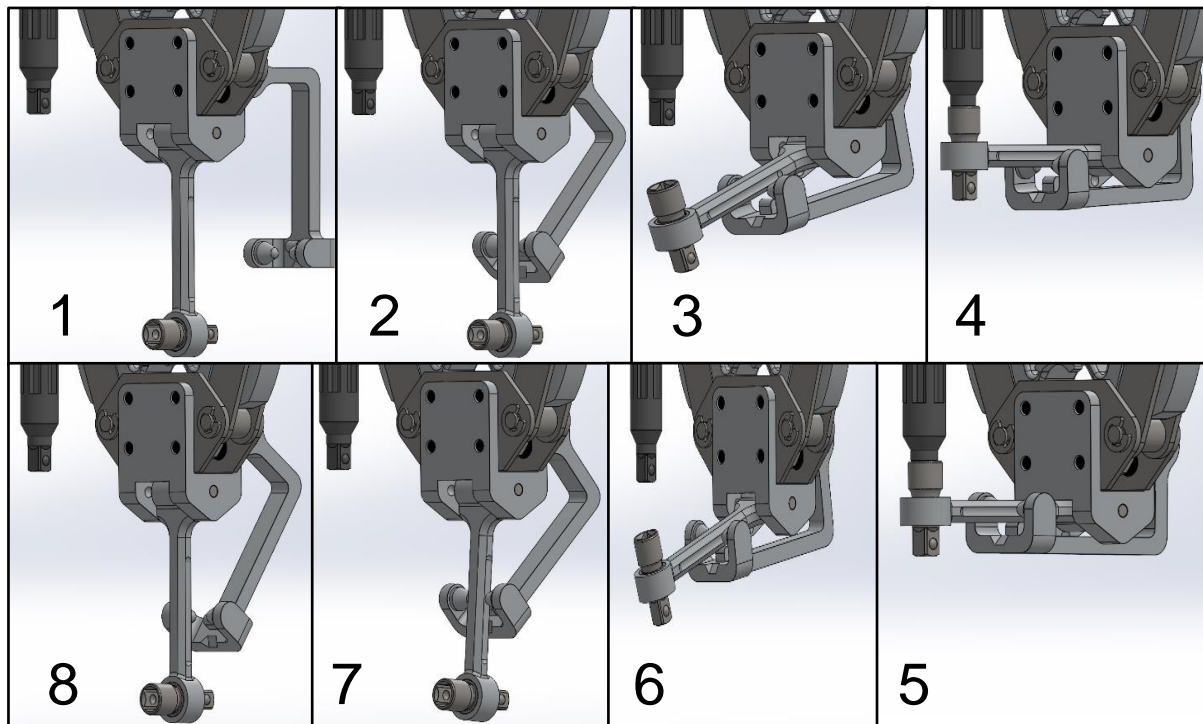


Figure 4: The diagram illustrates the tool change cycle, with steps 1-5 showing the clockwise motion of the swing arm as it transitions from the disengaged to the engaged position, and steps 6-8 depicting the transition from engaged to the disengaged position

The critical dimension for this mechanism is the length of the tool arm, which must be greater than the radius of the arc created by the clearance between the square socket and the screwdriver's plug. This ensures that the turning arc is shallow enough to fit within the available clearance on one side between the square plug and socket, allowing for smooth engagement and disengagement of the tool. A structural drawing of tool arm is illustrated in Figure 5. The maximum clearance between this 3/8-inch socket set is 0.28mm based on ASA B5.38-1958. [14]

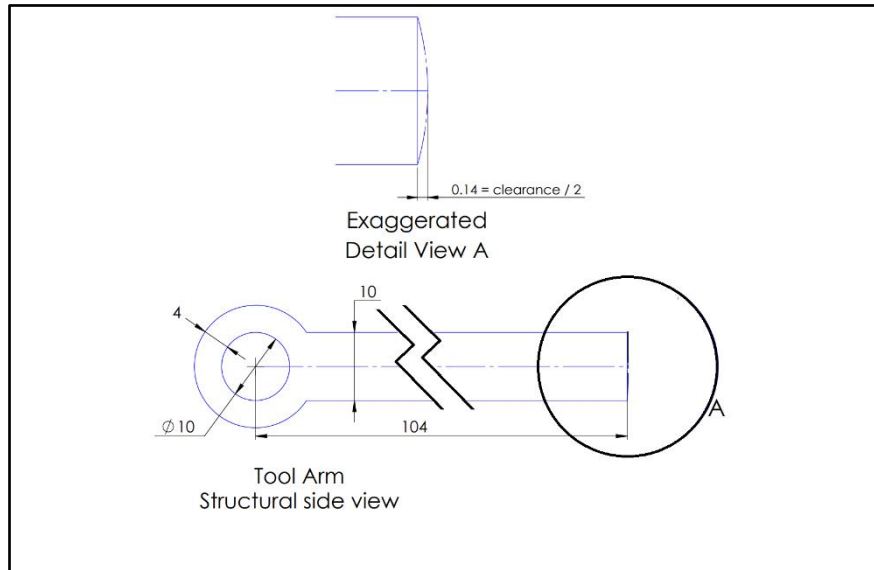


Figure 5: Structural drawing of tool arm with detailed view on top

2.2 MATERIAL SELECTION

Material selection is based on the following requirements:

- The tool changer must securely hold and change tools, maintaining rigidity and alignment with the screwdriver's spindle. The material used must provide sufficient strength to ensure structural integrity and support the necessary tolerances for precise and consistent tool positioning.
- The tool holder experiences low to moderate stresses from holding tools, with frequent movements during tool changes. The swing arm is subjected to moderate dynamic loading due to its rotational movements and the engagement and disengagement of tools. The chain mechanism, on the other hand, requires wear resistance.
- The material must withstand the robotic disassembly cell's environment, including minor temperature variations and exposure to lubricants or dust, without encountering extreme temperatures or chemicals.
- Materials must be machinable and suitable for precision components like the tool holder, swing arm, sprockets, and chain links. Press-fit applications require tight tolerances.

For each component of the chain magazine tool changer, the following material candidates are selected based on required properties:

- **Aluminum Alloy (6061 or 7075)** is ideal for the attachment, sprocket, tool arm, and swing arm due to its lightweight, machinability, strength, and corrosion resistance. It provides sufficient durability and precision for moderate-strength applications.
- **Carbon Steel or Stainless Steel** is chosen for high-wear components such as the chain links, and Geneva mechanism. These materials offer high strength, excellent wear resistance, and durability.
- **Brass** is used for press-fit bushings due to their self-lubricating properties and slim profile, ensuring smooth and low-maintenance operation.

2.3 ASSEMBLY

The assembly consists of two sprockets mounted on individual shafts, with one sprocket connected to the Geneva mechanism for tool advancement and the other acting as an idler. The drive wheel of the Geneva mechanism is powered by a DC motor, which rotates the sprocket and moves the chain to the desired position.

The chain is composed of alternating inner and attachment links. The rollers engage with the sprocket, while the pins secure the links. The attachments, which are machined from aluminium, are screwed onto the attachment links using M6 machine screws. These attachments hold the tool arms, which are mounted via dowel pins and self-lubricating bushings for smooth movement.

Each tool arm is fitted with a 3/8-inch square socket extension, mounted using needle roller bearings to allow free rotation. Various tools are attached to these sockets for different tasks. The swing arm is position near the lower sprocket, ensuring that the ball bearings align with the horizontal slots in the tool arm. The parallel distance between the axis of rotation of tool arm and the plane of rotation of sprocket is 45mm. This alignment helps guide the tool arm during its engagement with the screwdriver spindle. The rotational alignment of the screwdriver's square plug with the square socket extension is achieved by gradually rotating the screwdriver during the engagement process. Detailed dimensions for assembly are given in Appendix A. Figure 6 shows CAD model of assembled tool changer along with exploded view. The assembly tree of the model along with components required is shown in Figure 7.

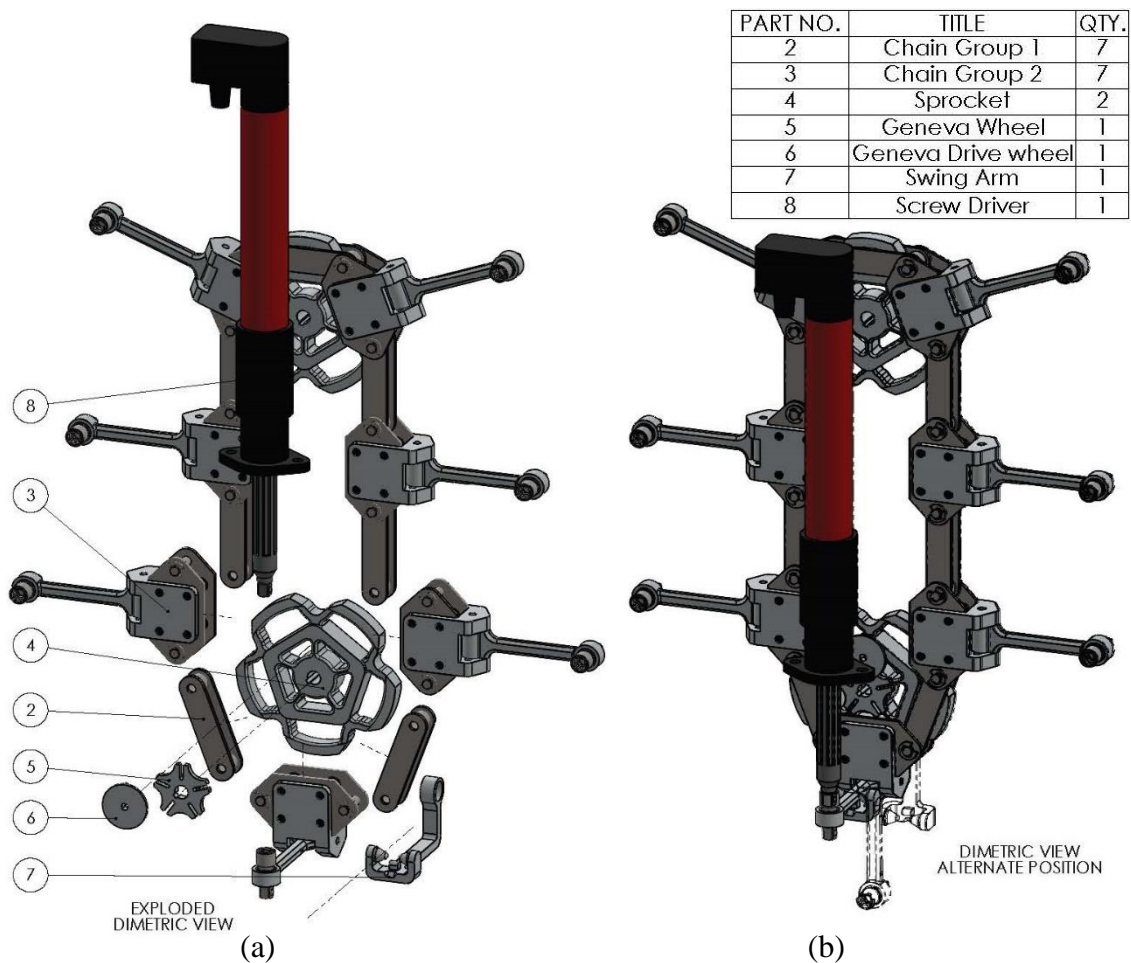


Figure 6: CAD image of assembly: (a) exploded view, (b) dimetric view

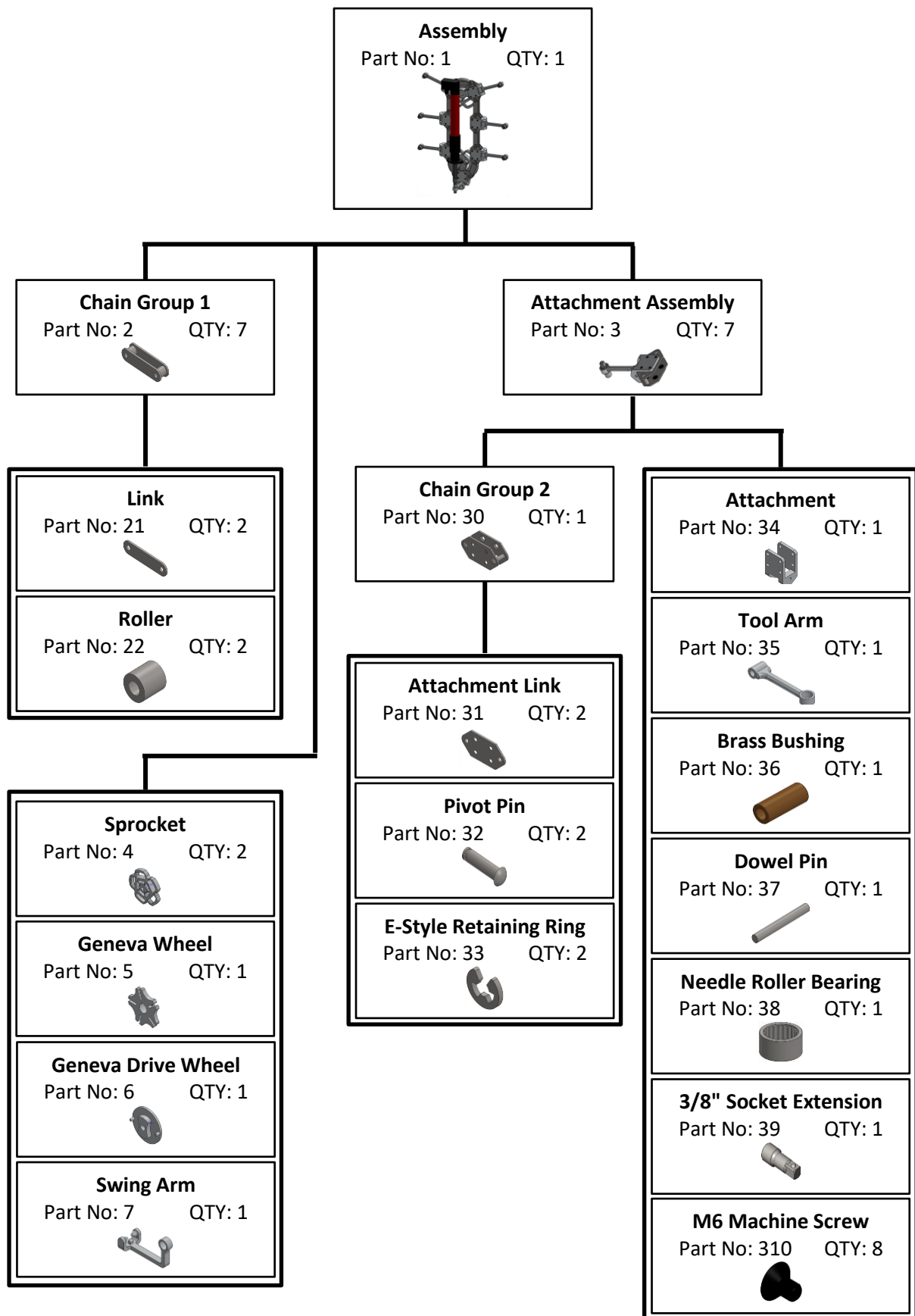


Figure 7: Assembly tree illustrating part number and quantity of each component

2.4 CONTROL SYSTEM INTEGRATION

To control the Geneva mechanism and the tool swing arm, a microcontroller-based control system is ideal. The microcontroller controls the rotation of the Geneva mechanism, ensuring the chain advances to the correct tool position, and also manages the actuation of the swing arm.

A simplified algorithm for the tool change process is outlined in the flowchart shown in Figure 8. The process starts by checking if the current tool is in use. If the correct tool is already in place, the program proceeds to completion. If the tool needs to be changed, the existing tool is swung off the drive shaft, the chain is rotated to the new tool position, and the new tool is then swung onto the drive shaft. Finally, the tool change is marked as complete, and the program ends.

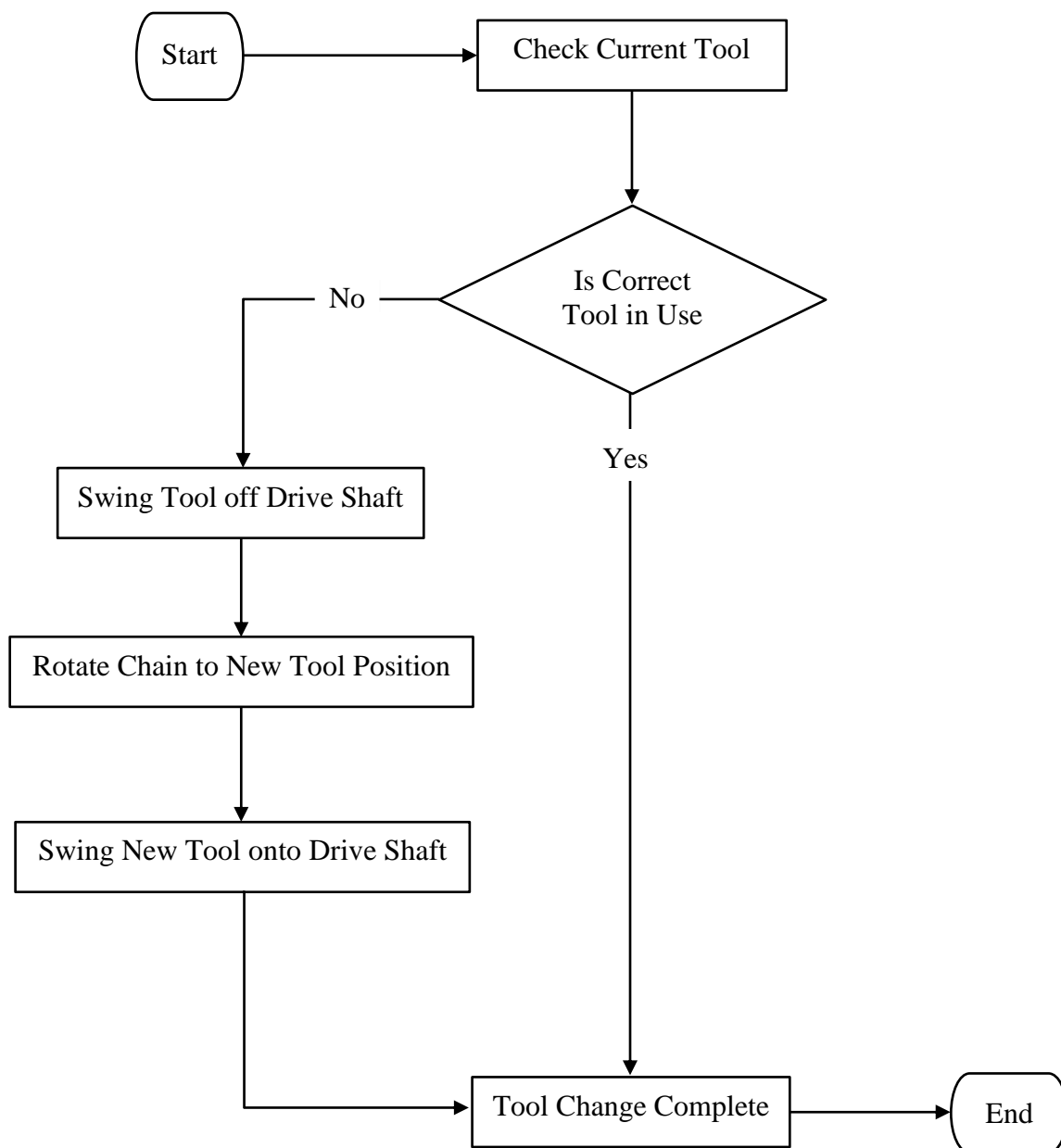


Figure 8: Flowchart illustrating the tool change algorithm

2.5 STRUCTURAL ANALYSIS

To validate the design's reliability, a detailed structural analysis was performed using SolidWorks Simulation. The following steps outline the process used to assess key components such as the tool arm, swing arm, attachment, chain links, and sprockets.

The model preparation and meshing process were applied uniformly to all components to ensure consistency in the analysis. Each component, including the tool arm, swing arm, chain links, and sprockets, underwent the same meshing protocol. However, the boundary conditions and load applications vary depending on the specific functionality and operational requirements of each component. These differences are outlined in the following sections to reflect the unique conditions each part of the tool changer experiences during operation.

2.5.1 Finite Element Analysis (FEA) Setup:

Model Preparation: The complete assembly, including the chain magazine, tool arm, swing arm, and sprockets, was imported into SolidWorks. Each component's material properties were assigned based on the previously selected materials (7075 aluminium for the tool arm, swing arm, sprockets and carbon steel for chain links, rollers and pivot pins).

Meshing: For the structural analysis of the model, a blended curvature-based mesh was used to ensure high accuracy, especially around complex geometries and curved surfaces. The following parameters were applied to achieve precise results:

- **Mesher:** Blended curvature-based mesh, which adapts element size according to the curvature of the model, ensuring finer mesh where needed.
- **Jacobian Points for High-Quality Mesh:** 16 points were used for Jacobian calculations, providing a high-quality mesh for improved accuracy in stress and displacement analysis.
- **Element Size:** A maximum element size of 2.5 mm was used, ensuring that larger, flat surfaces were adequately meshed without unnecessary refinement. While minimum element size was kept to 0.12 mm, allowing for finer mesh in critical areas like joints and contact points, ensuring accurate stress distribution calculations.
- **Mesh Quality:** High, to ensure the integrity and accuracy of the simulation results.

2.5.2 Tool Arm

The tool arm's boundary conditions were set to accurately simulate the real-world forces and constraints it experiences during operation. The following boundary conditions were applied:

- **Mounting on Cylindrical Bushing:** A fixed cylindrical constraint was applied at the location where the tool arm is mounted on the press-fit brass bushing. This simulates the rotational pivot point while allowing for rotation about the bushing's axis. The constraint limits the tool arm's movement in all directions except for the intended rotational movement.
- **Load Application:** A force load of 10 N from the bottom was applied to simulate the load exerted by the swing arm as it engages during the screwing/unscrewing process. This load was applied uniformly across the chamfered area where the swing arm makes contact with the tool arm.
- **Opposing Force:** An opposite force of 10N was applied at the point where the tool arm connects with the screwdriver spindle. This force simulates pressure exerted by the spindle during tool engagement. The force direction is opposite to the load applied from the bottom, representing the counteracting forces during the operation.

2.5.3 Swing Arm

The boundary conditions for the swing arm are given below:

- **Mounting on a Cylindrical Shaft:** A fixed cylindrical support was applied at the base where the swing arm is mounted on the shaft. This boundary condition allows rotational movement around the shaft's axis but constrains translational movement in all other directions. This reflects the pivoting action of the swing arm during tool engagement and disengagement.
- **Force Applied at the Business End:** A force of 10 N was applied at the business end of the swing arm. This simulates the force required to push the tool arm onto the screwdriver spindle. The force acts perpendicularly to the swing arm at the point of contact with the tool arm, simulating the actual interaction during operation.
- **Rotational Actuation by Servo Motor:** A rotational torque was applied to the cylindrical surface of the swing arm, representing the torque generated by the servo motor to rotate the arm. The servo motor applies a torque of 0.97 Nm, corresponding to the 97 mm length of the swing arm, to rotate the swing arm and push the tool arm into engagement with the screwdriver spindle. The opposing torque generated by the servo motor was applied to counteract the 10N force required to push the tool arm onto the spindle. This torque provides sufficient force to complete the tool engagement.

2.5.4 Attachment

The boundary conditions for the attachment, which is a machined aluminium part connected to the chain link, were set to simulate the forces and constraints it experiences during operation. The following conditions were applied:

- **Fixed Support at Mounting Points:** A fixed support constraint was applied at the locations where the attachment is secured to the chain link using eight M6 machine screws. This boundary condition restricts movement in all directions at these points, accurately replicating the attachment's fixed connection to the chain.
- **Load from the Tool Arm:** A force load of 10 N was applied at the location of the press-fit bushing where the tool arm is mounted, accounting for the tool changing forces and combined weight of the tool arm, attachment, and tool itself, with a maximum tool weight of 255 grams. This load includes 5 N downwards force to represent the gravitational force and an additional 5 N sideways to simulate forces exerted during tool handling.

2.5.5 Chain Link

The boundary conditions for the attachment chain link, which is a standard chain link with screw holes for securing the attachment, were set to simulate the operational forces it experiences during use. The following conditions were applied:

- **Fixed Support at the Pins:** Fixed support constraints were applied at the chain link pins, where the link is connected to adjacent links in the chain. These constraints allow the link to rotate around the pin but restrict translational movement in all other directions. This replicates the real-world behaviour of the chain during motion.
- **Tension in the Chain:** A tensile force 45 N was applied along the length of the chain link to simulate the tension generated in the chain due to the combined weight of the chain and the attached tool assembly. This force is applied through the pins at both ends of the attachment link, reflecting the forces acting on the chain during operation.

- **Load from the Tool Attachment:** A force load 10 N was applied at the screw holes where the tool attachment is secured. This represents the downward load exerted by the weight of the tool arm, tool, and attachment, ensuring that the interaction between the chain link and the attached components is captured.

2.5.6 Sprocket

The boundary conditions for the sprocket were defined to simulate its operational environment, where it is mounted on a shaft and drives the chain. The following boundary conditions were applied:

- **Fixed Support at the Shaft Mount:** A fixed support constraint was applied at the central hole of the sprocket, where it is mounted on the shaft. This restricts all translational movements while allowing rotational freedom around the shaft's axis, simulating how the sprocket is mounted and rotates during operation.
- **Torque Application:** A rotational torque of 1.45 Nm (calculated based on a pitch radius of 63.8 mm and a chain weight of 22.8 N) was applied specifically to the three engaged teeth, rather than distributing it across all teeth, to accurately simulate the force required to rotate the chain. Applying torque to all teeth would distribute the load unrealistically and could lead to incorrect results.
- **Chain Tension Force:** A tensile force 42 N was applied along the points of contact between the sprocket teeth and the chain, representing the tension in the chain as it wraps around the sprocket. This force accounts for the load exerted by the weight of the chain.

3 RESULTS

The structural analysis of key components was performed using SolidWorks Simulation to validate the design of the tool changer. Components analysed included the tool arm, swing arm, attachment, chain links, and sprockets. The simulation focused on stress, strain, and displacement to ensure the design's reliability under operational loads.

For the aluminium components (7075-O), with a yield strength of $3.0 \times 10^7 \text{ N / m}^2$ [15], the maximum observed stress for tool arm was $2.119 \times 10^6 \text{ N / m}^2$, well below the yield strength. For carbon steel, which has a minimum yield strength of $2.5 \times 10^8 \text{ N / m}^2$ [16], the maximum observed stress for swing arm was $2.746 \times 10^7 \text{ N / m}^2$. These results confirm that the material selection and design geometry are appropriate.

The maximum elastic deformation observed in the tool arm and swing arm, critical components of the tool changer, was $2.095 \times 10^{-2} \text{ mm}$ and $1.467 \times 10^{-1} \text{ mm}$, respectively. These deformations are acceptable given the mechanism's millimetre-level precision. The simulation study, along with the stress, strain, and displacement models for the tool arm and swing arm, is shown in Figure 9.

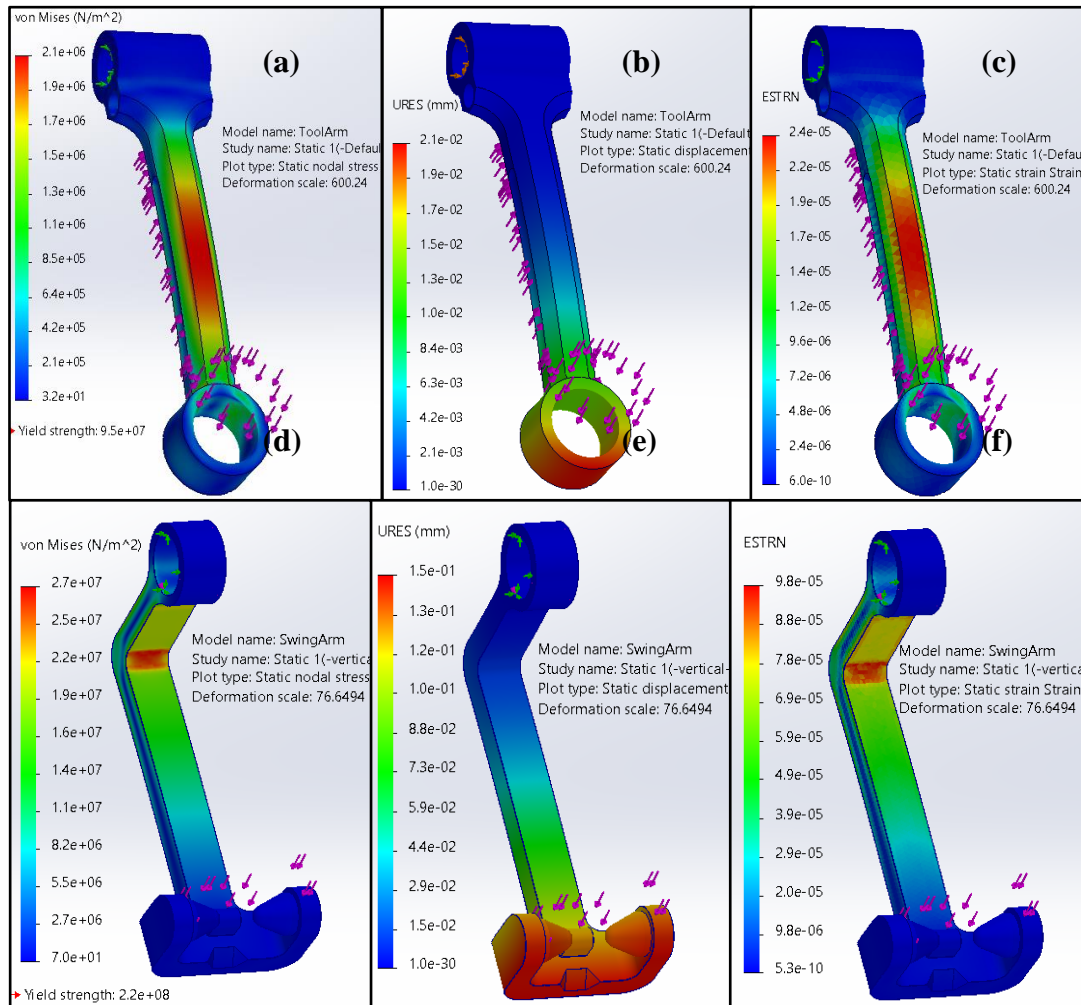


Figure 9: Simulation results of tool arm and swing arm: (a) stress on tool arm, (b) displacement of tool arm, (c) strain on tool arm, (d) stress on swing arm, (e) displacement of swing arm, (f) strain on swing arm

For attachment made of aluminium (7075-O), with a yield strength of $3.0 \times 10^7 \text{ N / m}^2$, the maximum recorded stress was $3.712 \times 10^5 \text{ N / m}^2$, which is significantly below the yield strength. Similarly, for the chain link made of carbon steel, with a yield strength of $2.5 \times 10^8 \text{ N / m}^2$, the maximum observed stress was $1.058 \times 10^7 \text{ N / m}^2$. These stress values further validate the suitability of the material selection and design.

The maximum elastic deformation observed in the attachment and chain link was $4.132 \times 10^{-5} \text{ mm}$ and $3.083 \times 10^{-3} \text{ mm}$, respectively, which are negligible given the mechanism's required precision. The simulation study, along with the stress, strain, and displacement models, is shown in Figure 10.

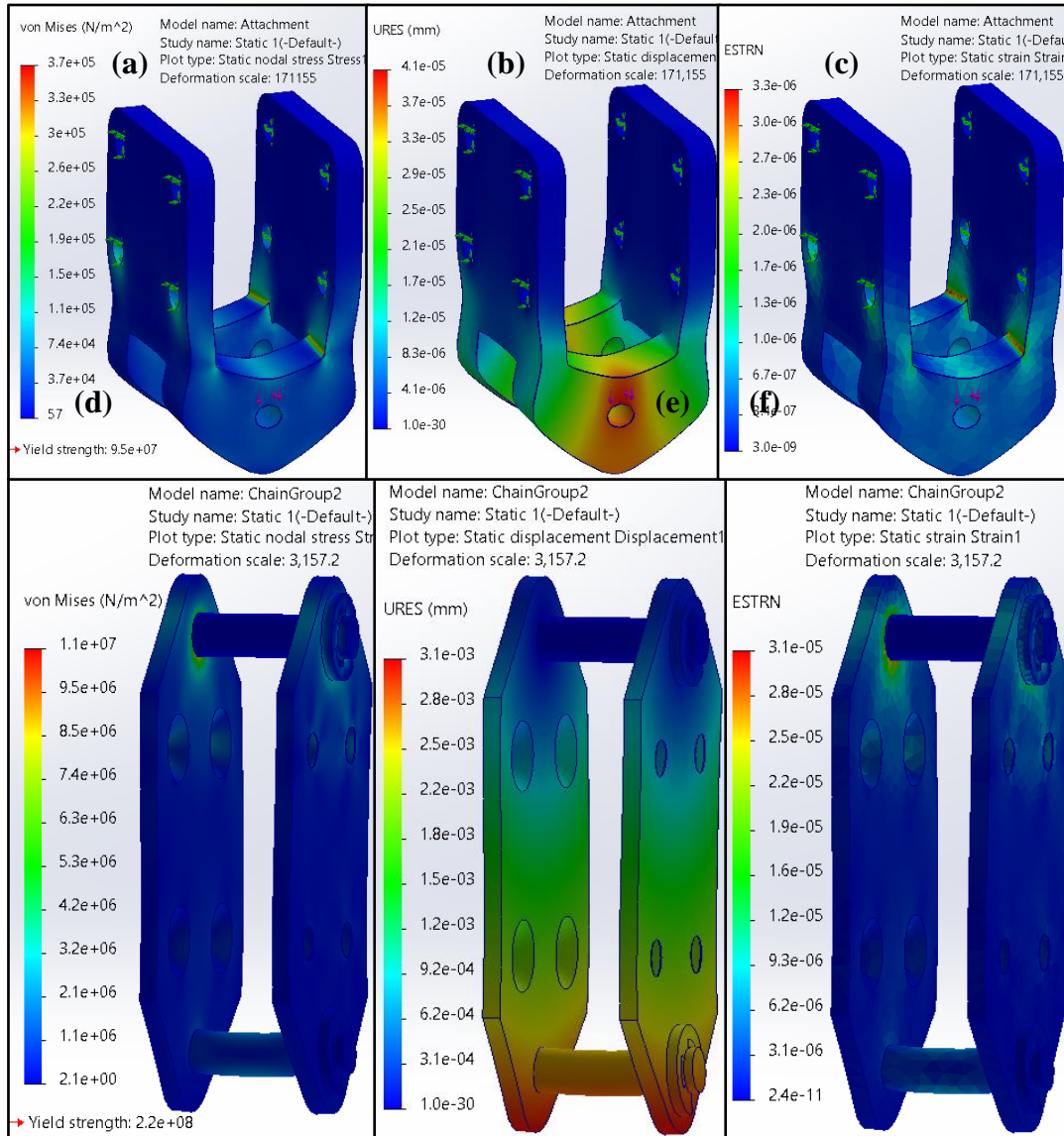


Figure 10: Simulation results of tool arm and swing arm: (a) stress on attachment, (b) displacement of attachment, (c) strain on attachment, (d) stress on chain link, (e) displacement of chain link, (f) strain on chain link

The results confirmed that the design can withstand the operational forces without significant deformation or failure. Noticed that applied stress is well below the yield point ensuring the material not plastically deformed, material will deform elastically and will return to its original shape. Detailed values of stress and displacement observed in all components is given in table provided in Appendix B.

The sprocket, constructed from aluminium (7075-O), has a yield strength of $3.0 \times 10^7 \text{ N / m}^2$, with the highest observed stress being $1.163 \times 10^7 \text{ N / m}^2$, well within safe limits. Under maximum load, the resulting elastic deformation was $1.469 \times 10^{-2} \text{ mm}$, which is insignificant relative to the size of the socket. The stress, strain, and displacement analysis for this component is illustrated in Figure 11.

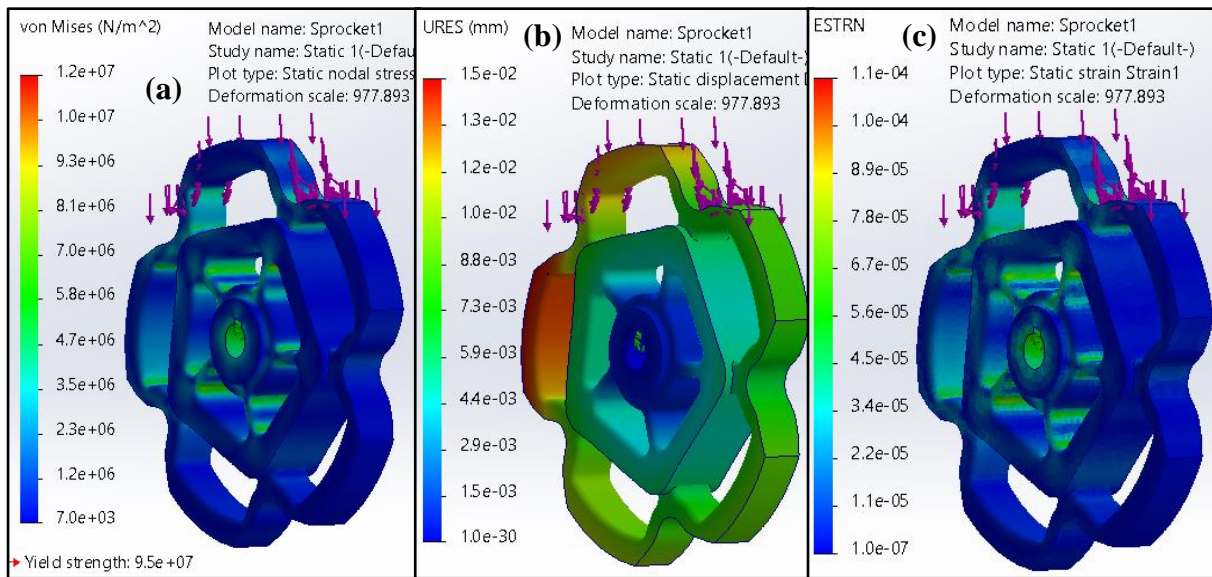


Figure 11: Simulation results of sprocket: (a) stress, (b) displacement, (c) strain

The overall analysis demonstrates that the chain magazine tool changer is structurally sound, with stress, strain, and displacement values all within acceptable limits. All stress values for the remaining components were also below their respective yield strengths, ensuring structural integrity during operation. Detailed stress values are provided in Appendix B.

4 DISCUSSION AND CONCLUSIONS

The primary objective of this report was to design bit changing mechanism and validate the structural integrity of components through Finite Element Analysis (FEA). Key components, including the tool arm, swing arm, attachment, and sprockets, were analysed for stress, strain, and displacement. The results show that all components are well within their material yield strengths, confirming the reliability of the design.

While the FEA results are promising, further research could focus on dynamic load conditions, fatigue analysis, and experimental validation of the simulation outcomes. One area of improvement could be the reduction in the weight of the attachment, which could be achieved through refined geometry or alternative materials. Furthermore, future research could explore the use of carbon fiber as a replacement material for the tool arm and swing arm, offering the possibility of additional weight reduction. These future studies would enhance the robustness of the design and ensure long-term reliability in varied operational environments.

In summary, the FEA results confirm that the current design and material selection meet the criteria for the tool changer. The structural integrity of the components has been verified, as all stress and deformation values remain within acceptable limits. The design meets the necessary criteria for reliability under operational loads. Further research could enhance the design by reducing weight and exploring alternative materials for key components.

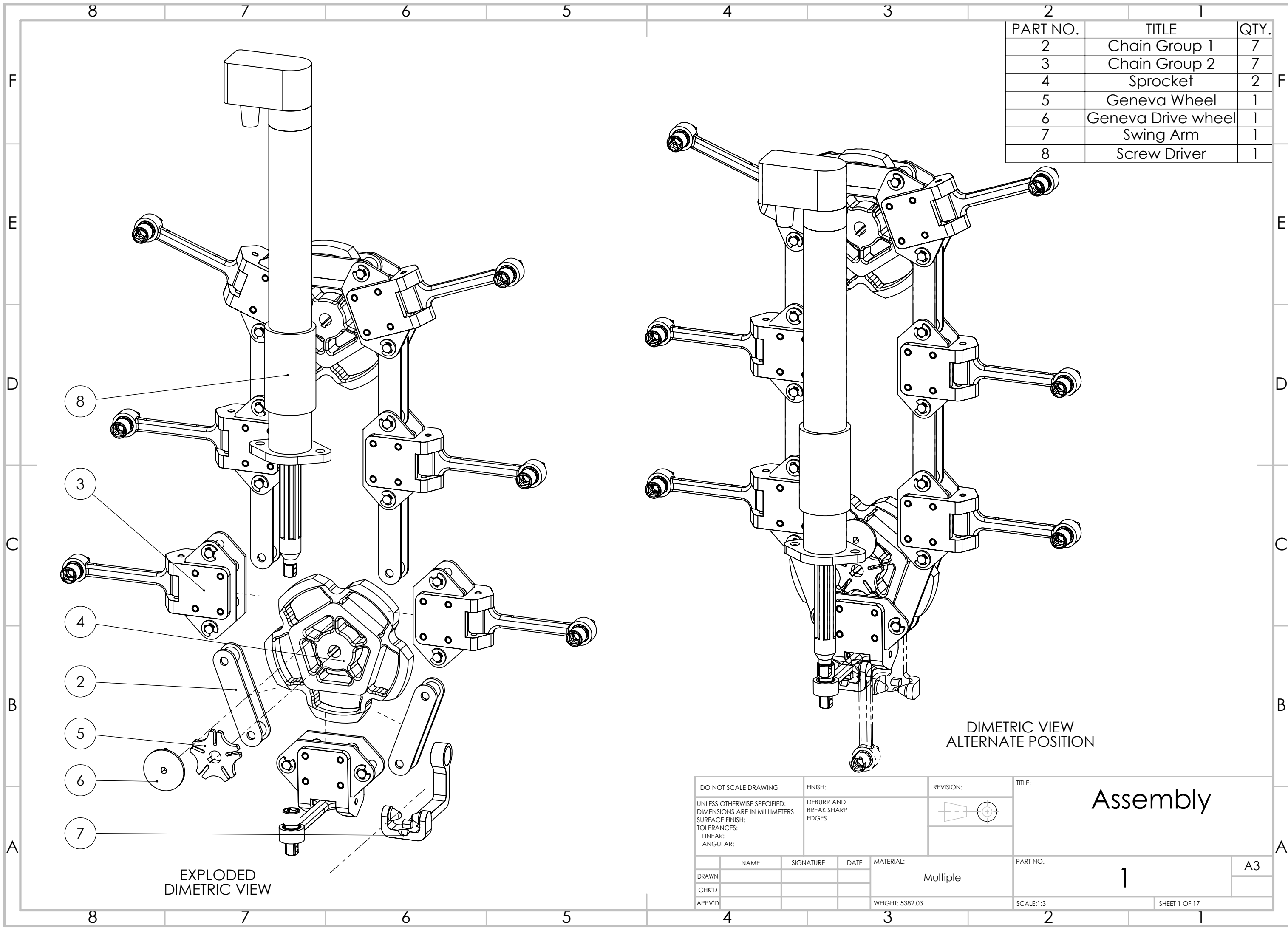
REFERENCES

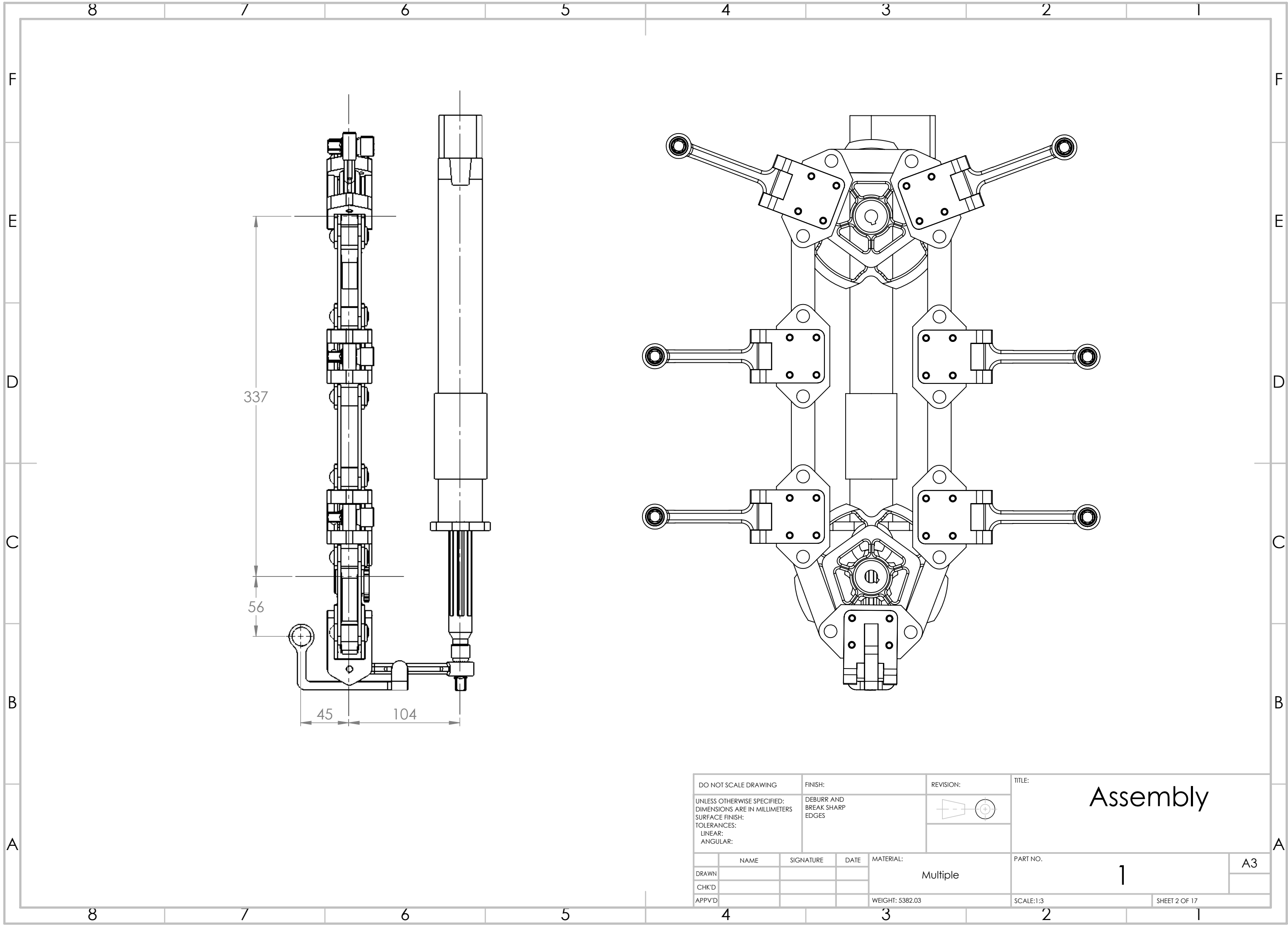
- [1] Kaarlela T, Villagrossi E, Rastegarpanah A, et al. Robotised disassembly of electric vehicle batteries: A systematic literature review. *J Manuf Syst* 2024; 74: 901–921.
- [2] Hathaway J, Contreras CA, Stolkin R, et al. Technoeconomic Assessment of Electric Vehicle Battery Disassembly -- Challenges and Opportunities from a Robotics Perspective. DOI: 10.2139/SSRN.4803459.
- [3] Lander L, Tagnon C, Nguyen-Tien V, et al. Breaking it down: A techno-economic assessment of the impact of battery pack design on disassembly costs. *Appl Energy* 2023; 331: 120437.
- [4] Beaudet A, Larouche F, Amouzegar K, et al. Key Challenges and Opportunities for Recycling Electric Vehicle Battery Materials. *Sustainability* 2020, Vol 12, Page 5837 2020; 12: 5837.
- [5] Gökler MI, Koç MB. Design of an automatic tool changer with disc magazine for a CNC horizontal machining center. *Int J Mach Tools Manuf* 1997; 37: 277–286.
- [6] McLaren I, Gorlach I. Development of a Tool Changer for a Reconfigurable Machine Tool. *Applied Mechanics and Materials* 2015; 798: 324–328.
- [7] Chen WH, Wegener K, Dietrich F. A robot assistant for unscrewing in hybrid human-robot disassembly. *2014 IEEE International Conference on Robotics and Biomimetics, IEEE ROBIO 2014* 2014; 536–541.
- [8] Rastegarpanah A, Ner R, Stolkin R, et al. Nut Unfastening by Robotic Surface Exploration. *Robotics* 2021, Vol 10, Page 107 2021; 10: 107.
- [9] Feldmann K, Trautner S, Meedt O. Innovative disassembly strategies based on flexible partial destructive tools. *Annu Rev Control* 1999; 23: 159–164.
- [10] Seliger G, Keil T, Rebafka U, et al. Flexible disassembly tools. *IEEE International Symposium on Electronics and the Environment* 2001; 30–35.
- [11] Wright J. *Standard Handbook of Chains: Chains for Power Transmission*. 2nd ed. Taylor & Francis Inc, <https://www.whsmith.co.uk/products/standard-handbook-of-chains-chains-for-power-transmission-and-material-handling-second-edition-mecha/american-chain-association/hardback/9781574446470.html> (2005, accessed 16 September 2024).
- [12] RF03075R-DT Detailed Information - Large Size Conveyor Chain DT Series, https://tt-net.tsubakimoto.co.jp/tecs/pdct/clc/pdct_Dtl_CLRFDt.asp?kata=RF03075R-DT (accessed 16 September 2024).
- [13] Lingaiah K, York N, San C, et al. *Machine Design Databook*. 2nd ed. McGraw-Hill Education, <https://www.accessengineeringlibrary.com/content/book/9780071367073> (2003, accessed 16 September 2024).
- [14] Oberg E, Jones FD. *Machinery's Handbook*. 28th ed. Industrial Press, Inc., <https://www.amazon.co.uk/Machinerys-Handbook-28th-Erik-Oberg/dp/0831128011> (2008, accessed 18 September 2024).
- [15] Ashby M. *Materials Selection in Mechanical Design*. 4th ed. Butterworth-Heinemann, 2011. Epub ahead of print 5 October 2011. DOI: 10.1016/C2009-0-25539-5.
- [16] Ashby M, Shercliff H, Cebon D. *Materials: engineering, science, processing and design*. 4th ed. Butterworth-Heinemann, 2018.

APPENDIX A

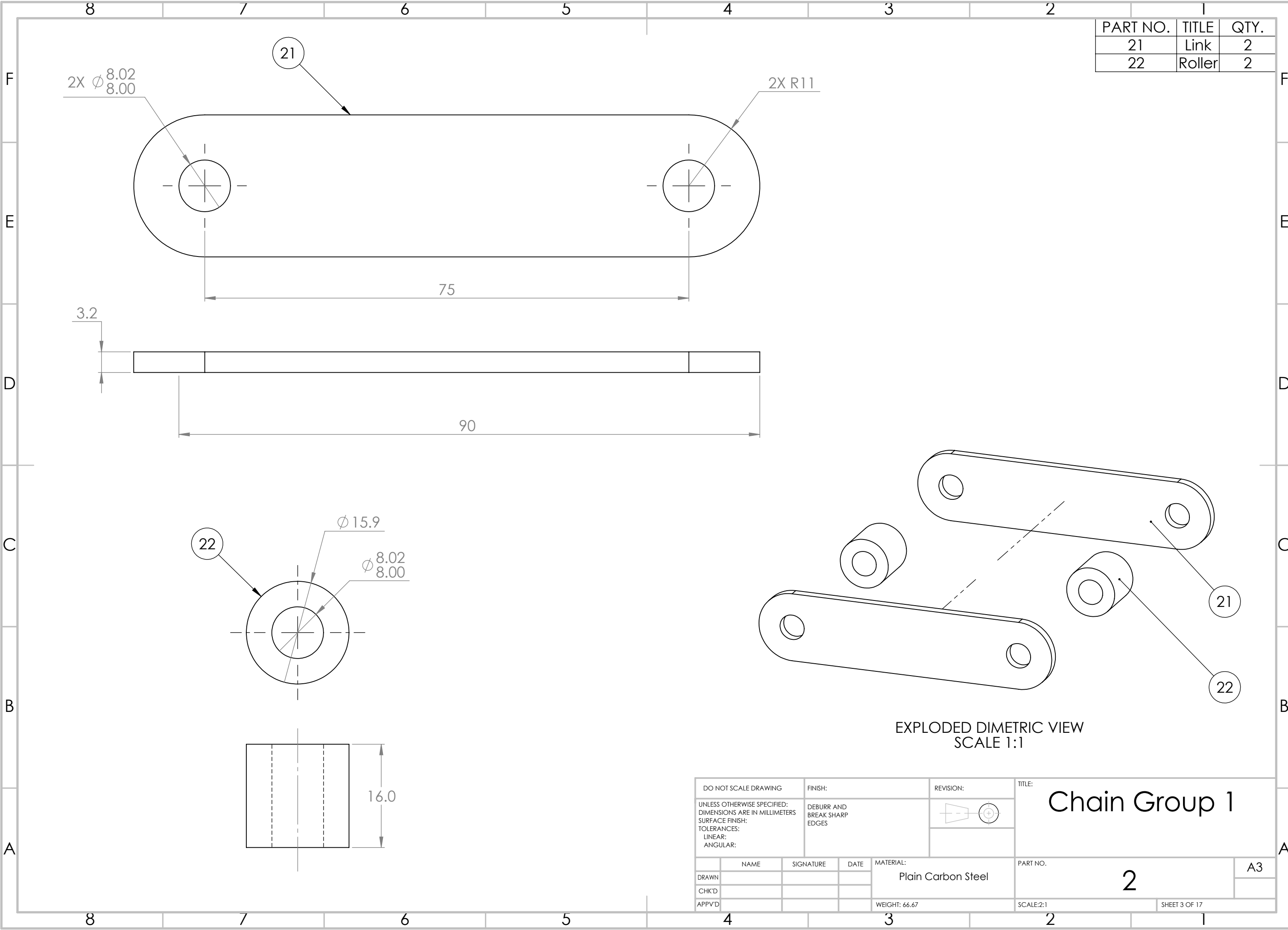
Detailed engineering drawing of all components are as follows:

Sheet 1	Assembly Exploded
Sheet 2	Assembly View
Sheet 3	Chain Group 1
Sheet 4	Chain Group 2
Sheet 5	Attachment Link
Sheet 6	Pivot Pin
Sheet 7	E-Style Retaining Ring
Sheet 8	Attachment
Sheet 9	Tool Arm
Sheet 10	Brass Bushing
Sheet 11	Dowel Pin
Sheet 12	Needle Roller Bearing
Sheet 13	3/8" Square Socket Extension
Sheet 14	Sprocket
Sheet 15	Geneva Wheel
Sheet 16	Geneva Drive wheel
Sheet 17	Swing Arm



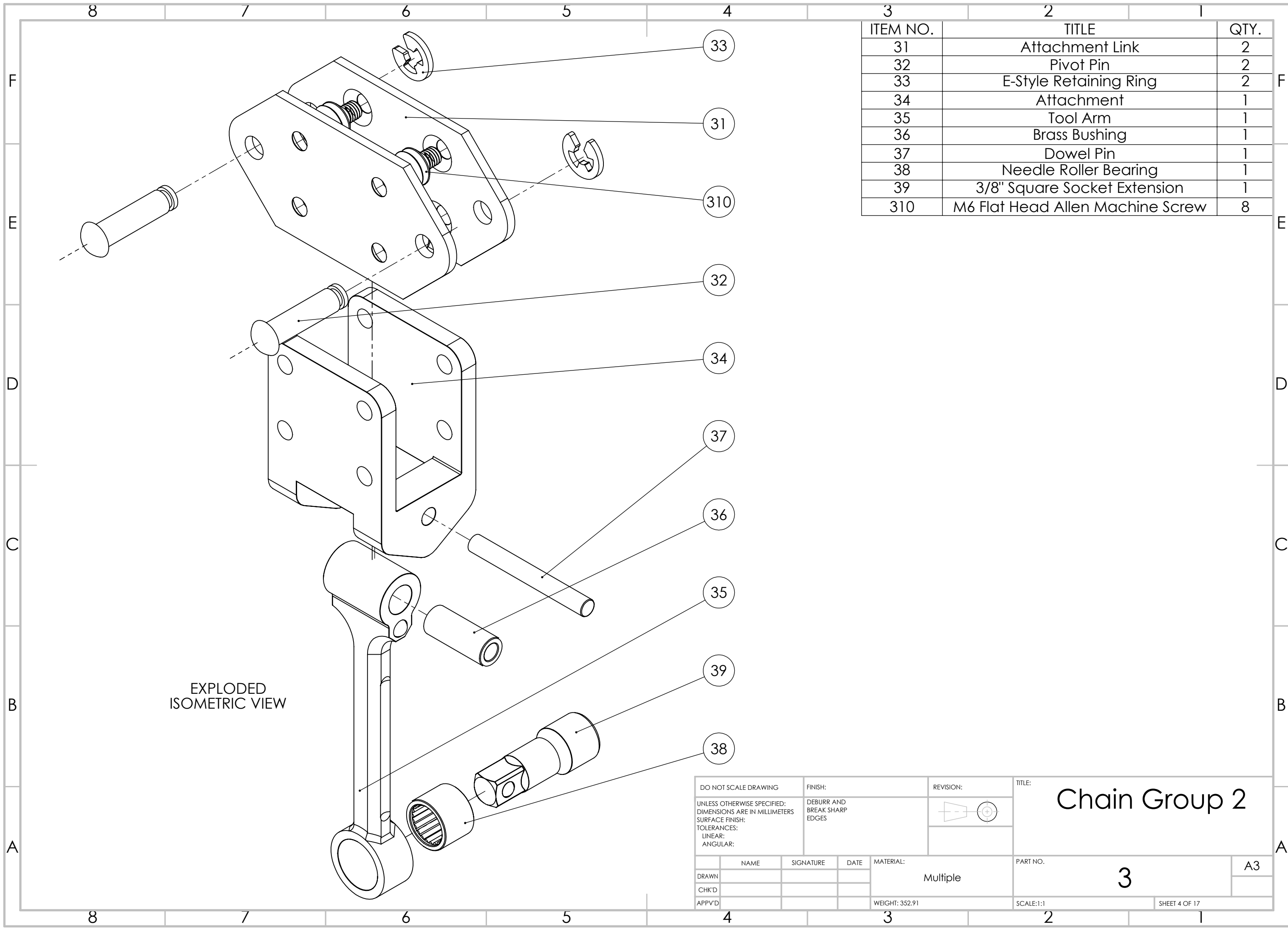


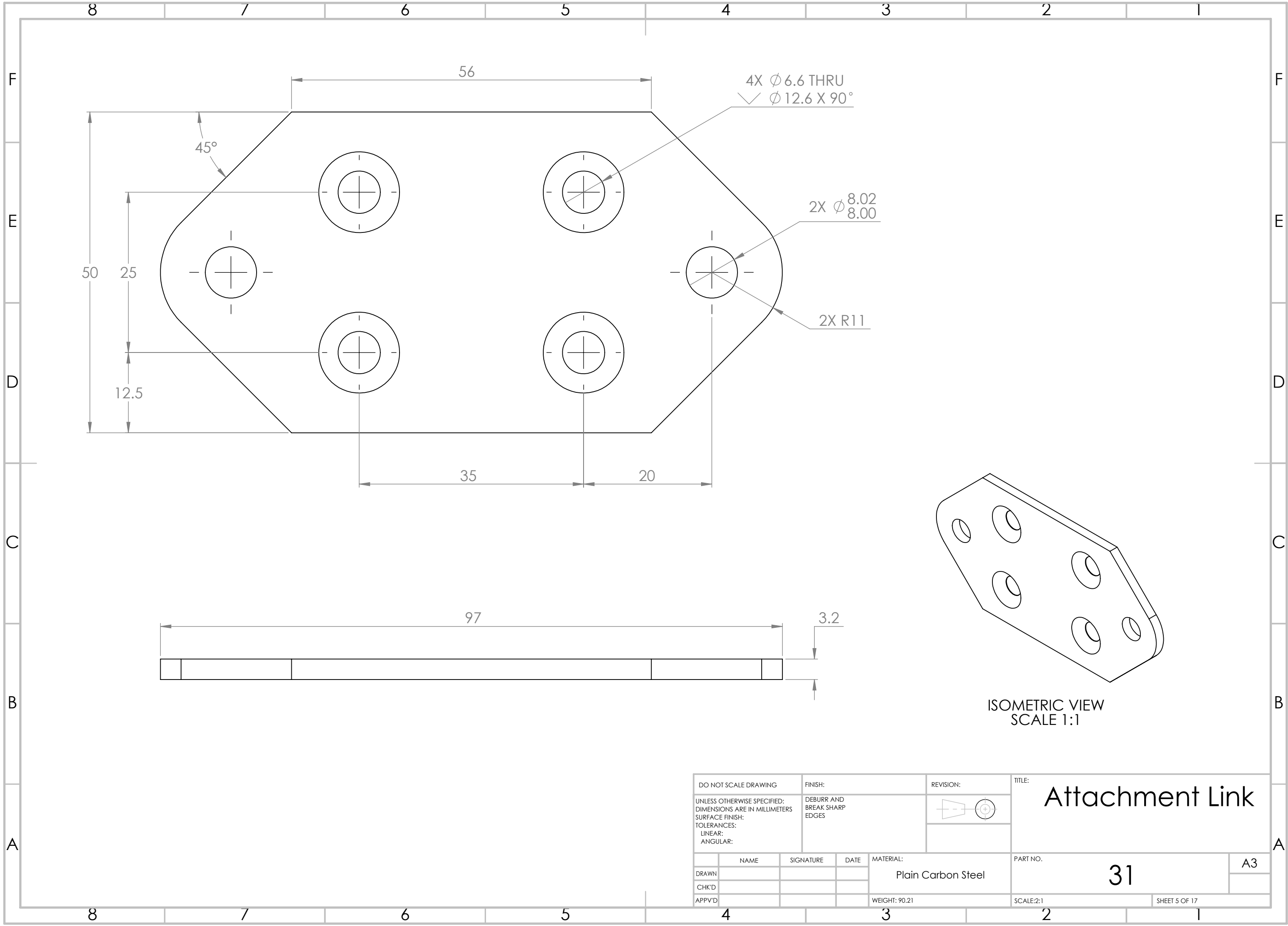
DO NOT SCALE DRAWING				FINISH:		REVISION:		TITLE:	
UNLESS OTHERWISE SPECIFIED: DIMENSIONS ARE IN MILLIMETERS SURFACE FINISH: TOLERANCES: LINEAR: ANGULAR:				DEBURR AND BREAK SHARP EDGES				Assembly	
	NAME	SIGNATURE	DATE	MATERIAL: Multiple		PART NO. 1		A3	
DRAWN									
CHK'D									
APPV'D				WEIGHT: 5382.03		SCALE:1:3		SHEET 2 OF 17	

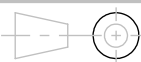


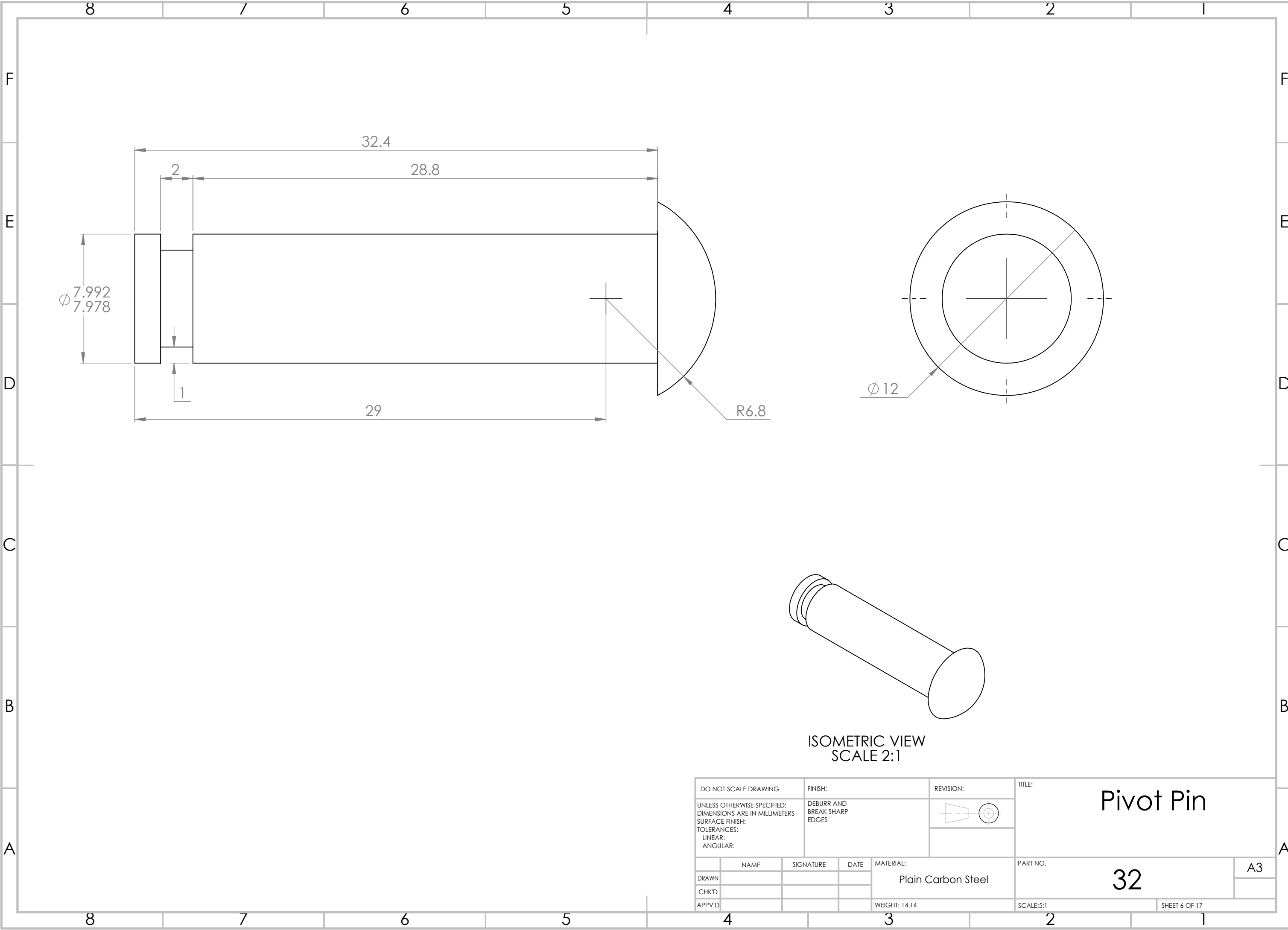
PART NO.	TITLE	QTY.
21	Link	2
22	Roller	2

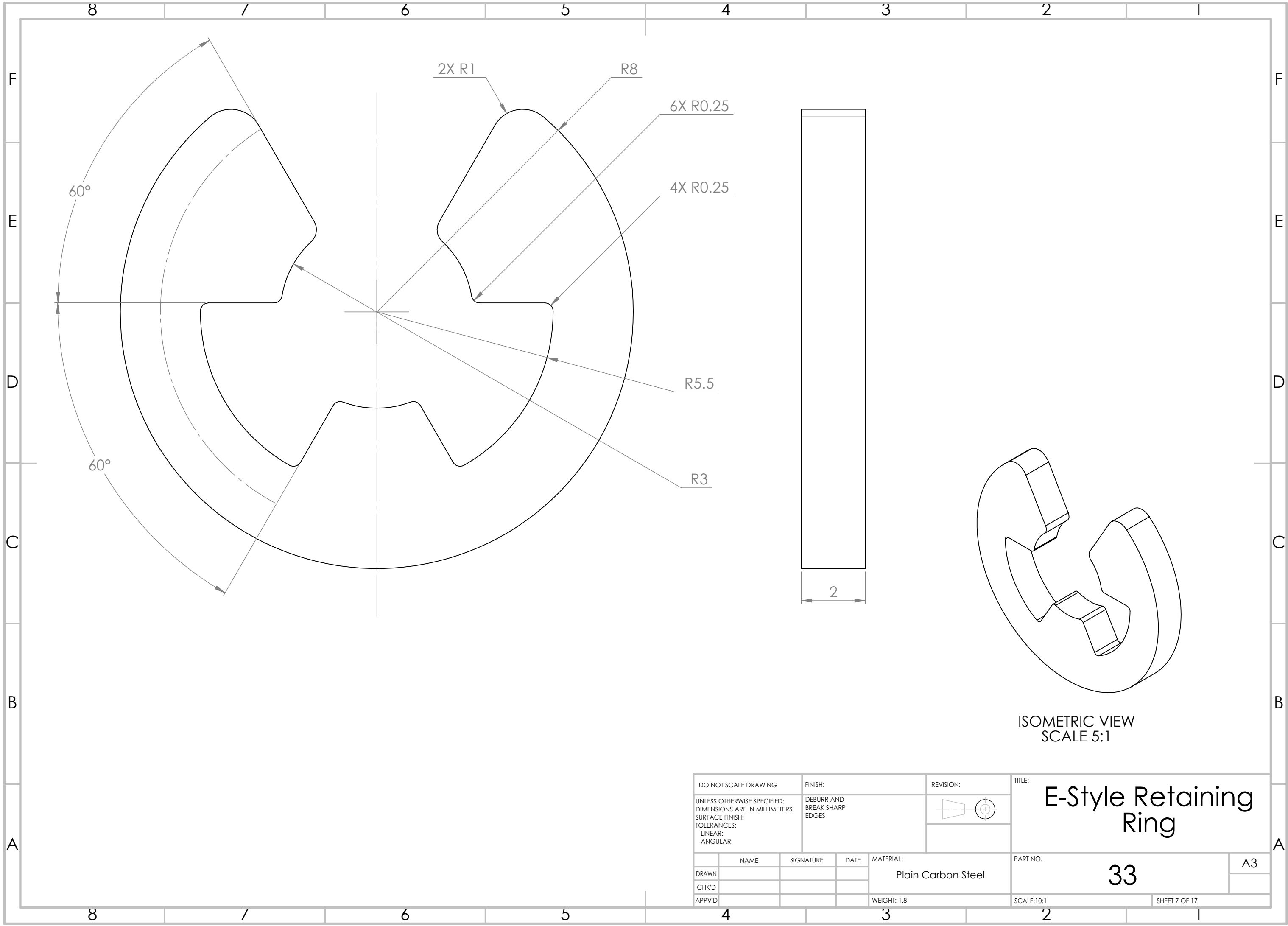
DO NOT SCALE DRAWING				FINISH:	REVISION:	TITLE:	
UNLESS OTHERWISE SPECIFIED: DIMENSIONS ARE IN MILLIMETERS SURFACE FINISH: TOLERANCES: LINEAR: ANGULAR:						Chain Group 1	
DRAWN	NAME	SIGNATURE	DATE	MATERIAL:		PART NO.	
CHK'D							
APPV'D				Plain Carbon Steel		2	
				WEIGHT: 66.67		SCALE: 2:1	
						SHEET 3 OF 17	

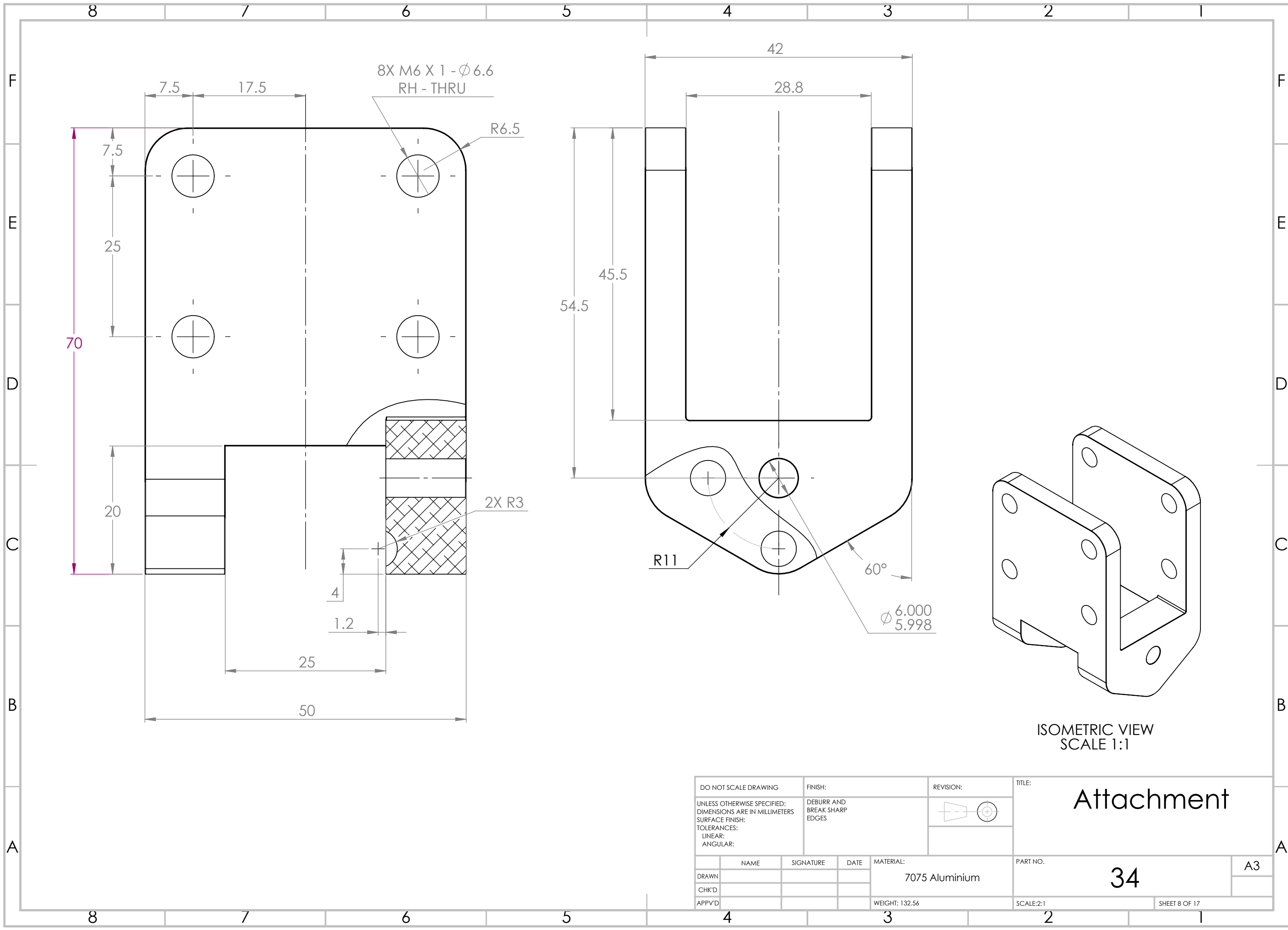


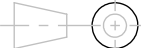


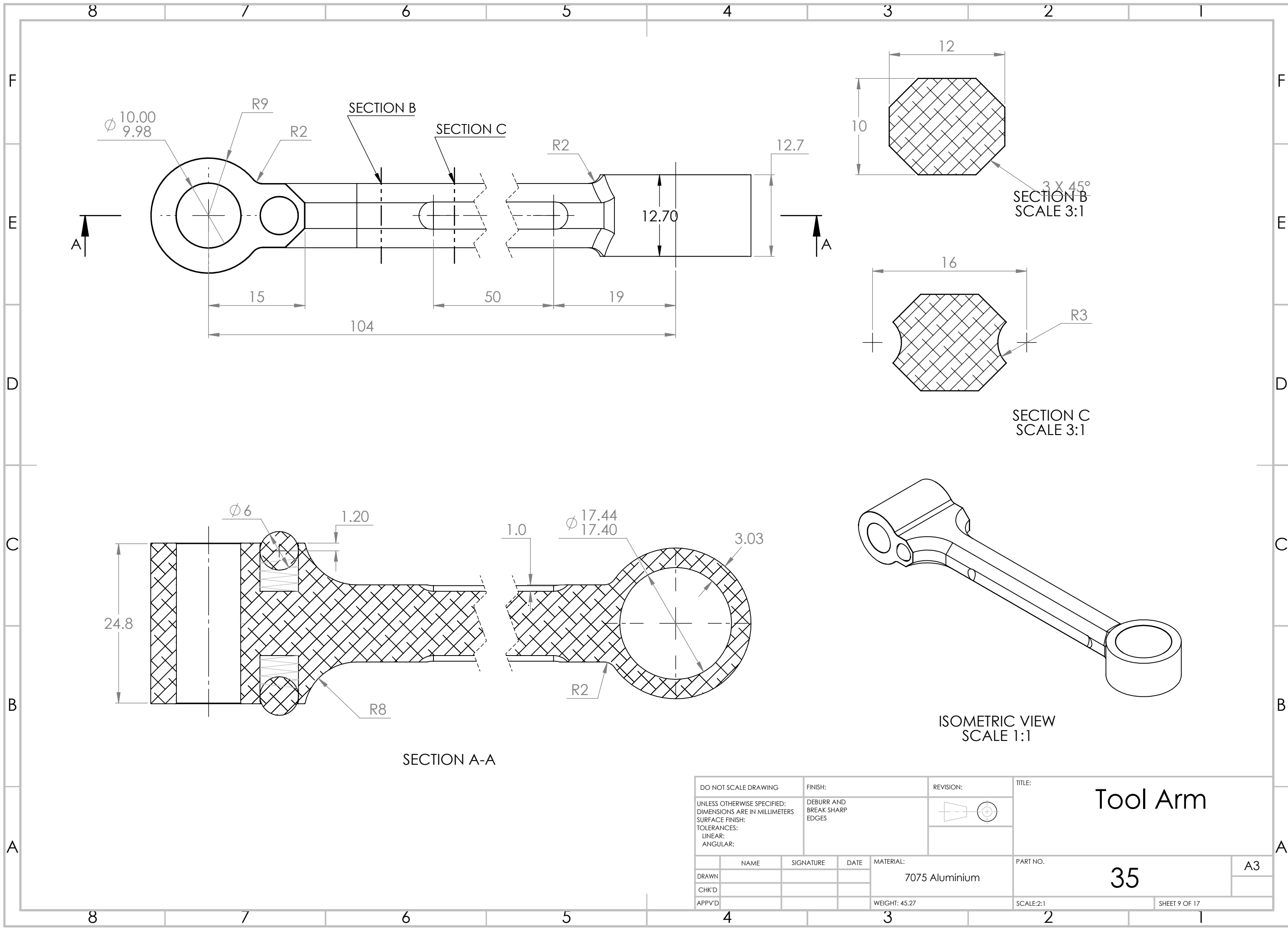
DO NOT SCALE DRAWING				FINISH: DEBURR AND BREAK SHARP EDGES		REVISION: 		TITLE: Attachment Link	
UNLESS OTHERWISE SPECIFIED: DIMENSIONS ARE IN MILLIMETERS SURFACE FINISH: TOLERANCES: LINEAR: ANGULAR:				MATERIAL: Plain Carbon Steel		PART NO. 31		A3	
DRAWN									
CHK'D									
APPV'D				WEIGHT: 90.21		SCALE: 2:1		SHEET 5 OF 17	

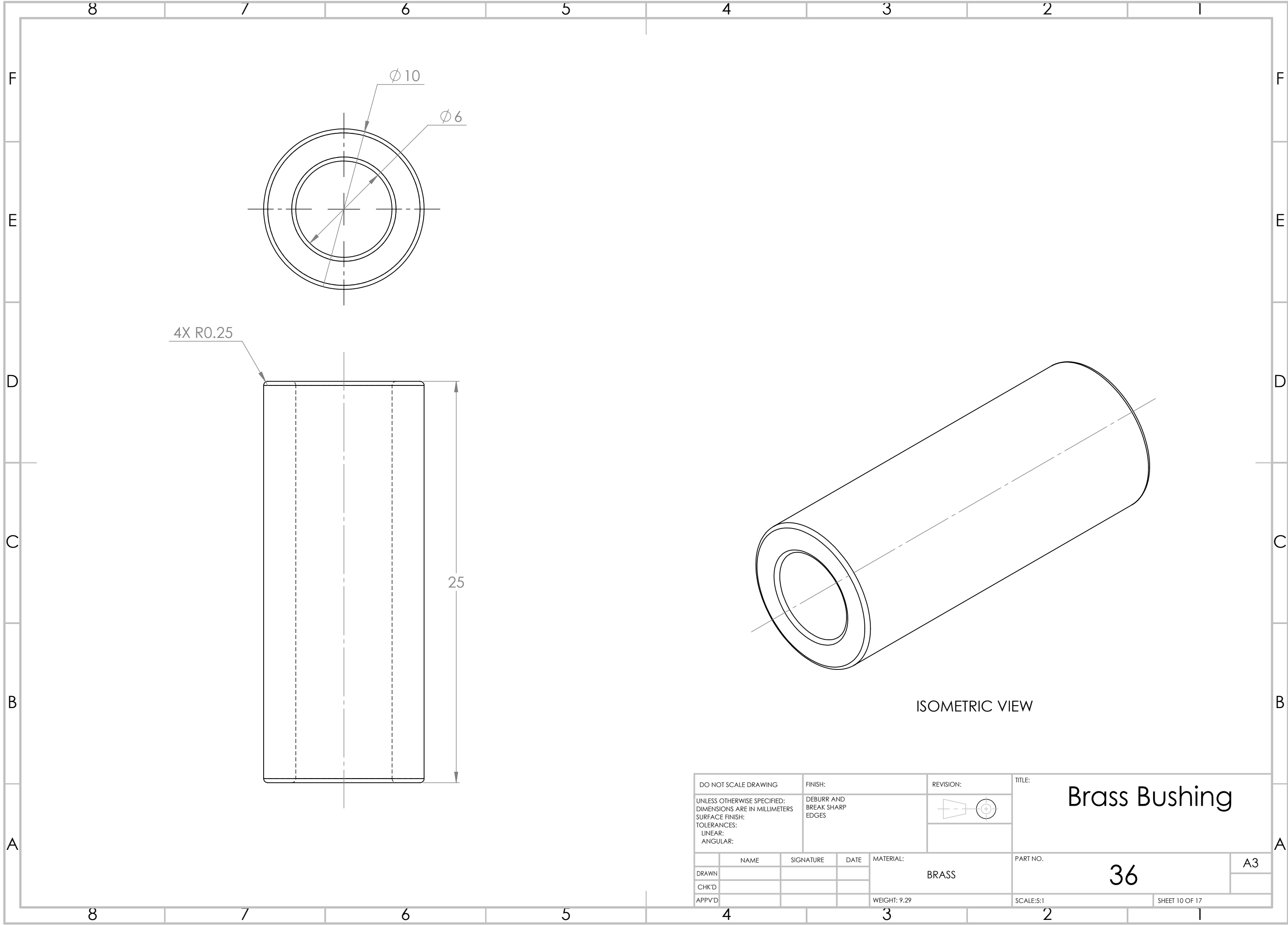


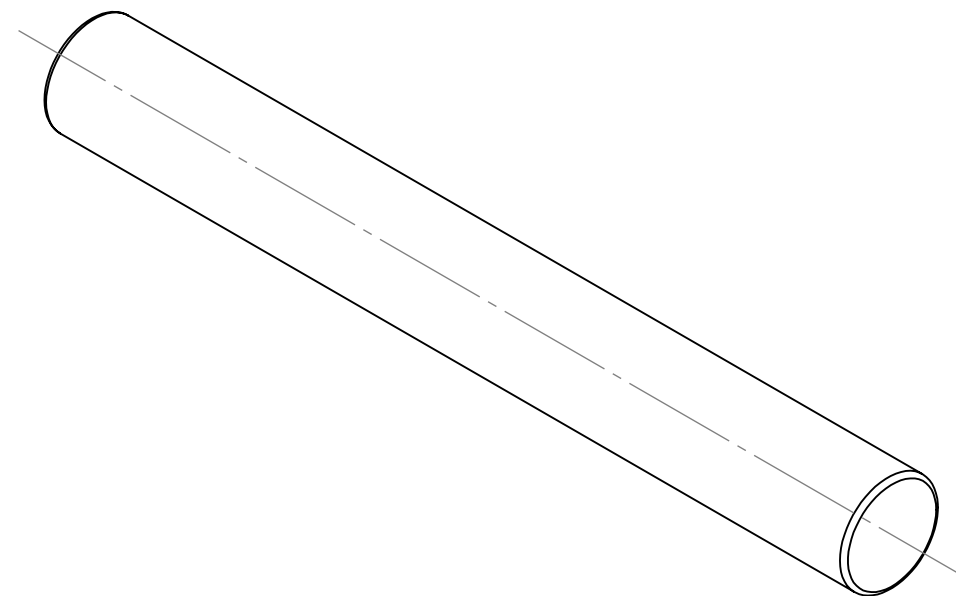
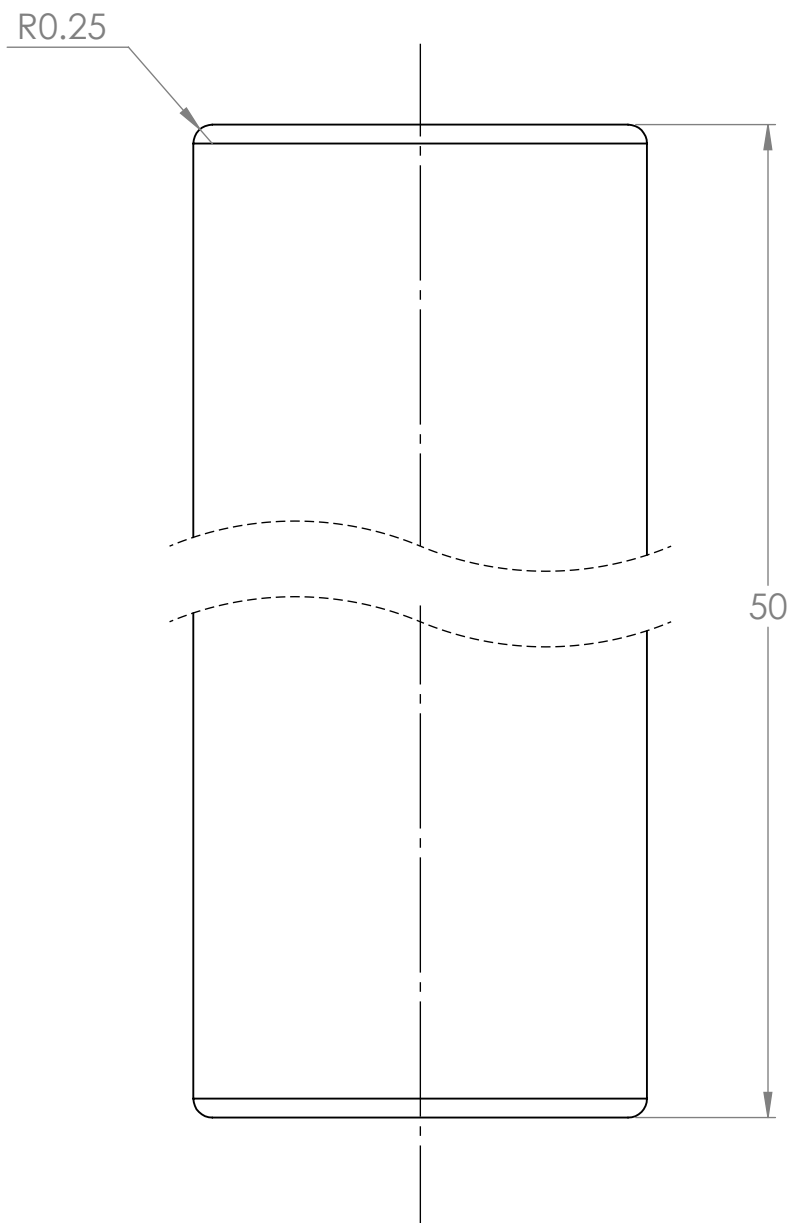
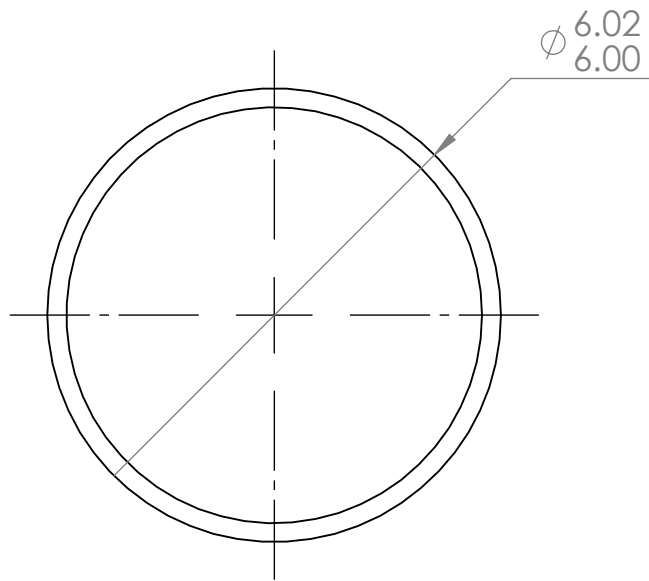




DO NOT SCALE DRAWING			FINISH:			REVISION:			TITLE:		
UNLESS OTHERWISE SPECIFIED: DIMENSIONS ARE IN MILLIMETERS SURFACE FINISH: TOLERANCES: LINEAR: ANGULAR:			DEBURR AND BREAK SHARP EDGES						Attachment		
	NAME	SIGNATURE	DATE	MATERIAL: 7075 Aluminium			PART NO. 34			A3	
DRAWN											
CHK'D											
APPV'D				WEIGHT: 132.56			SCALE:2:1			SHEET 8 OF 17	

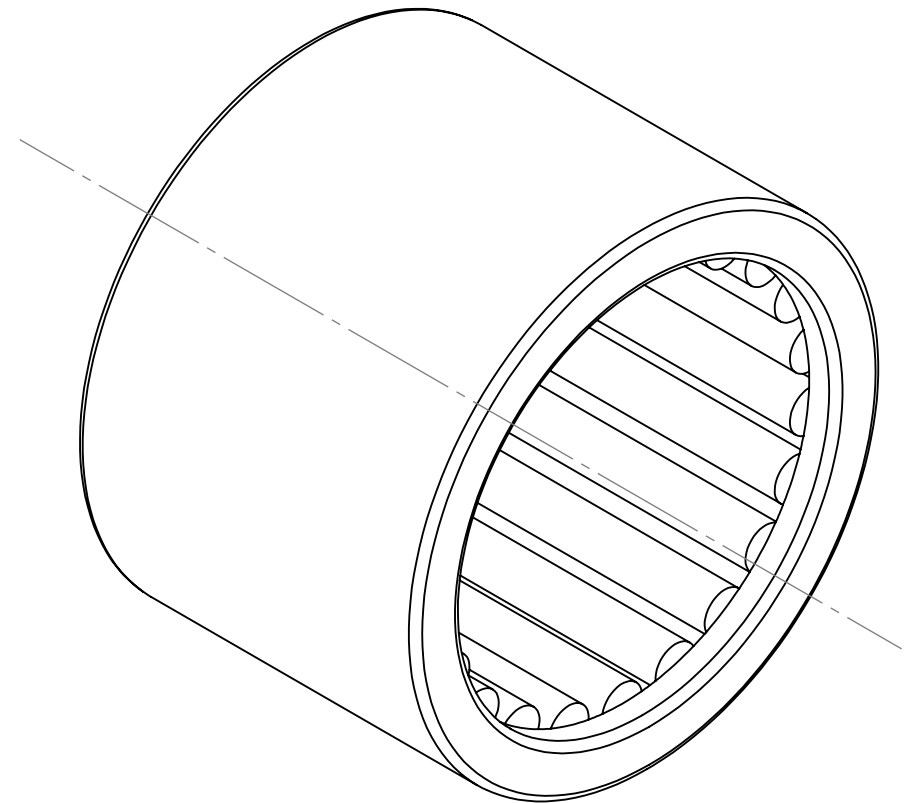
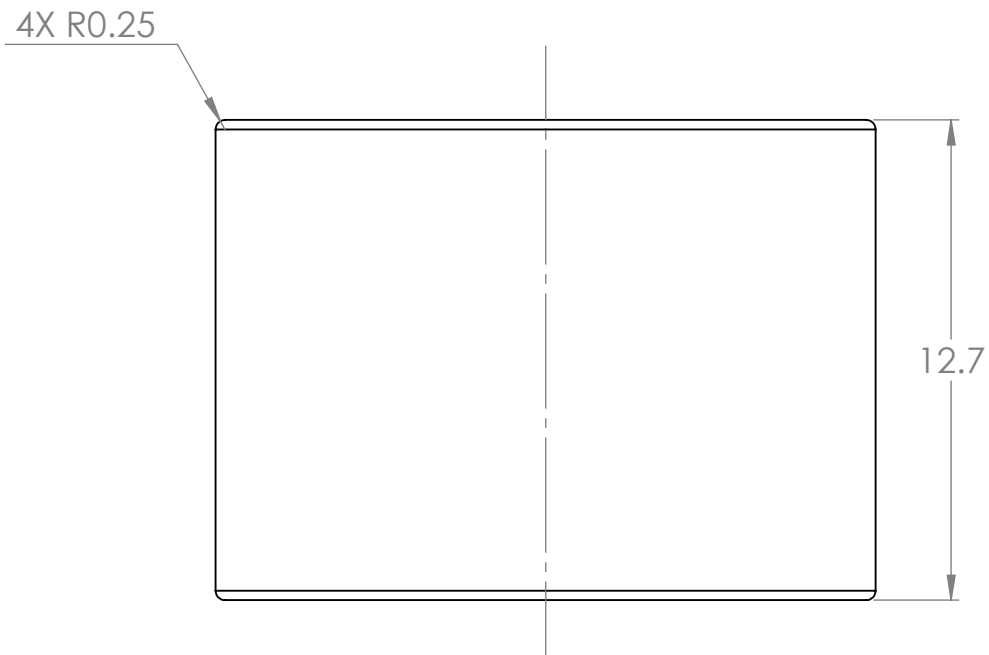
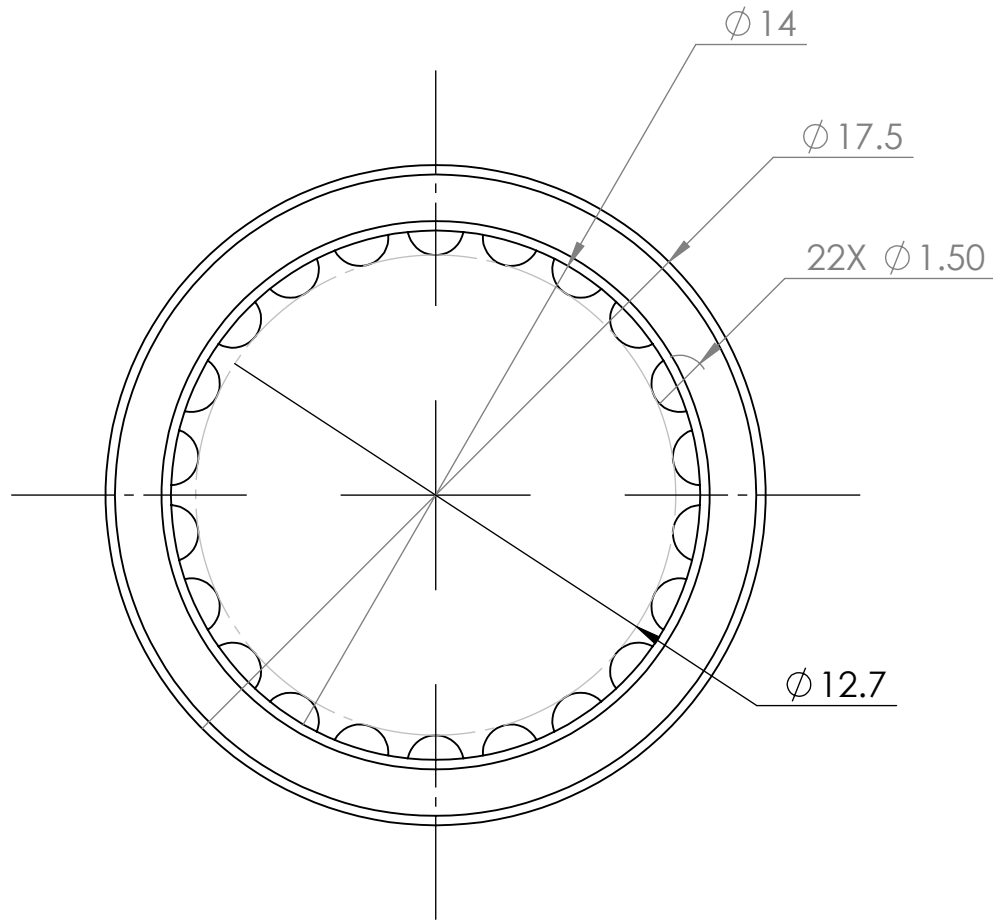






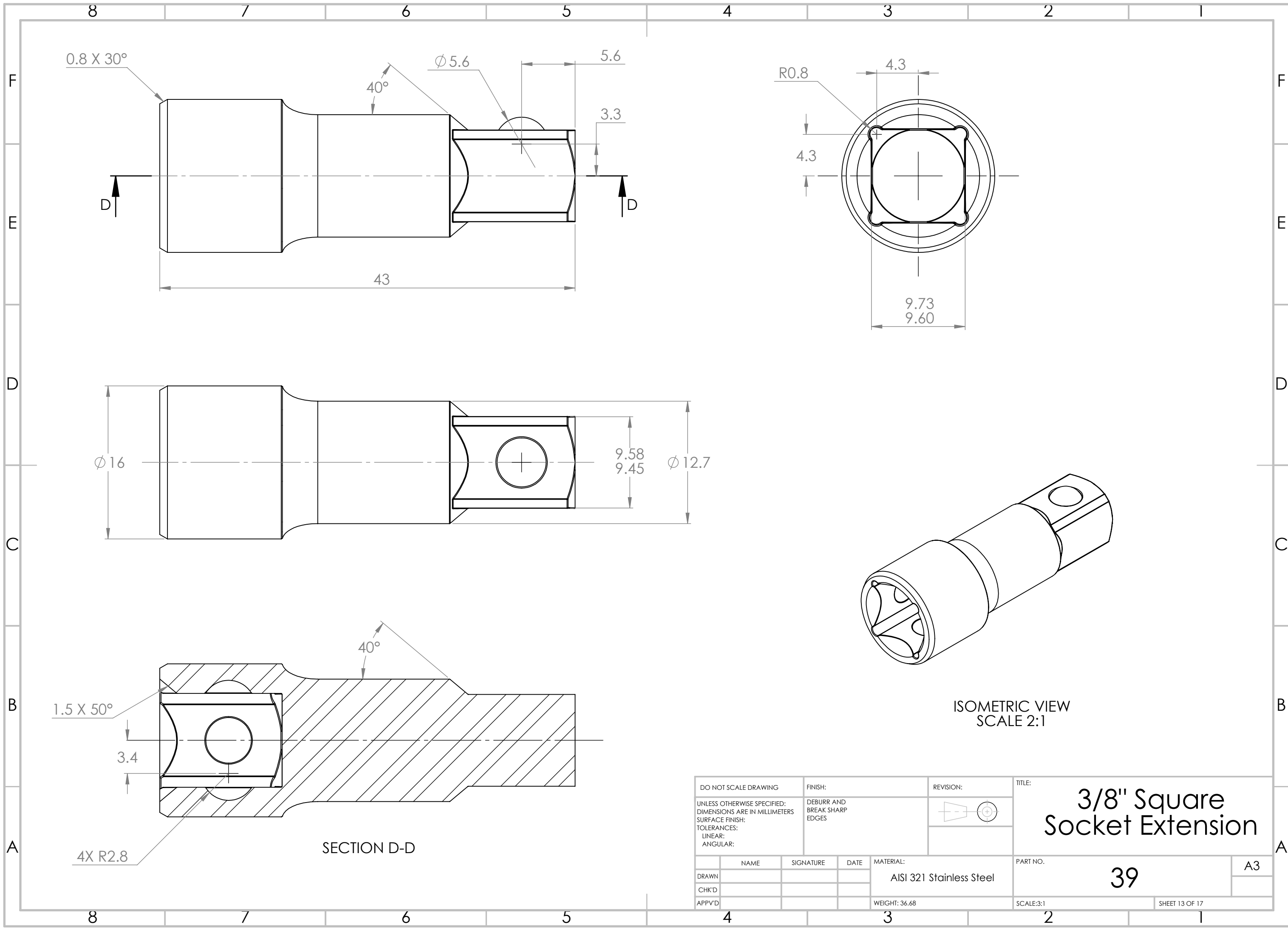
ISOMETRIC VIEW
SCALE 3:1

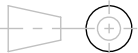
DO NOT SCALE DRAWING		FINISH:		REVISION:		TITLE:	
UNLESS OTHERWISE SPECIFIED: DIMENSIONS ARE IN MILLIMETERS SURFACE FINISH: TOLERANCES: LINEAR: ANGULAR:		DEBURR AND BREAK SHARP EDGES				Dowel Pin	
	NAME	SIGNATURE	DATE	MATERIAL:		PART NO.	A3
DRAWN				Plain Carbon Steel		37	
CHK'D				WEIGHT: 11.02		SCALE:10:1	
APPV'D						SHEET 11 OF 17	

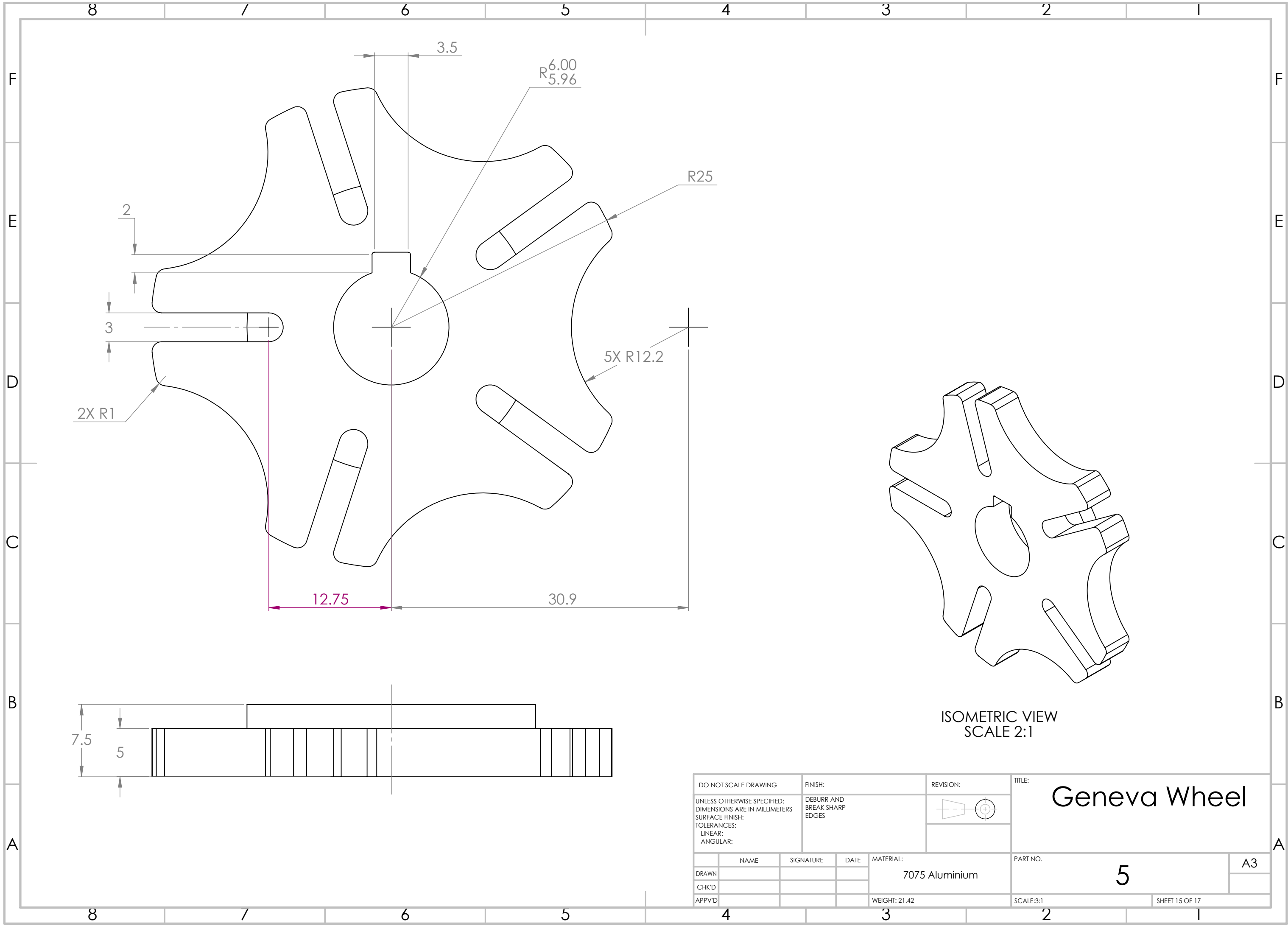


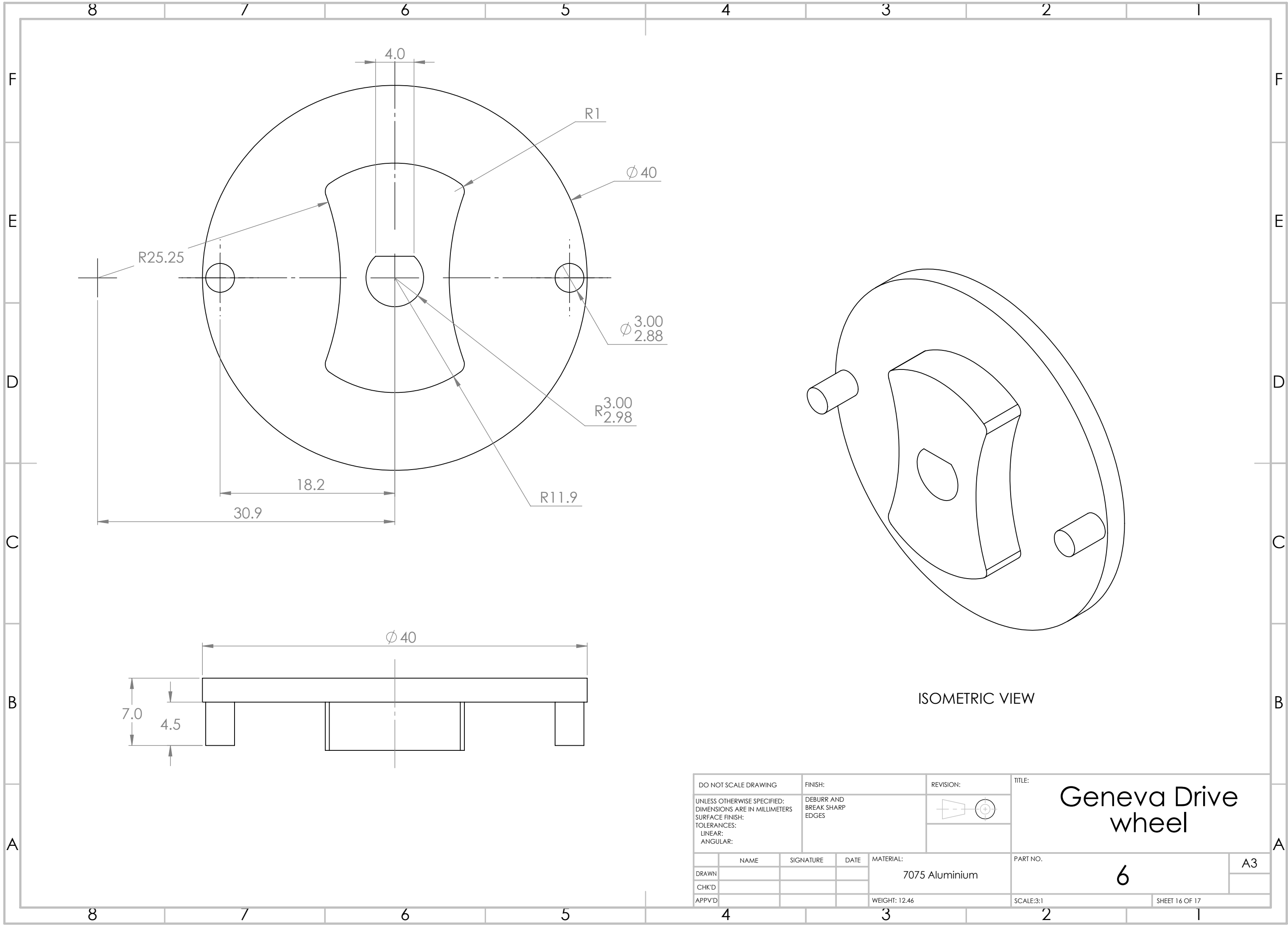
ISOMETRIC VIEW

DO NOT SCALE DRAWING		FINISH:		REVISION:		TITLE:	
UNLESS OTHERWISE SPECIFIED: DIMENSIONS ARE IN MILLIMETERS SURFACE FINISH: TOLERANCES: LINEAR: ANGULAR:		DEBURR AND BREAK SHARP EDGES				Needle Roller Bearing	
	NAME	SIGNATURE	DATE	MATERIAL:			
DRAWN				AISI 321 Stainless Steel		38	A3
CHK'D							
APPV'D				WEIGHT: 8.93			SCALE:5:1

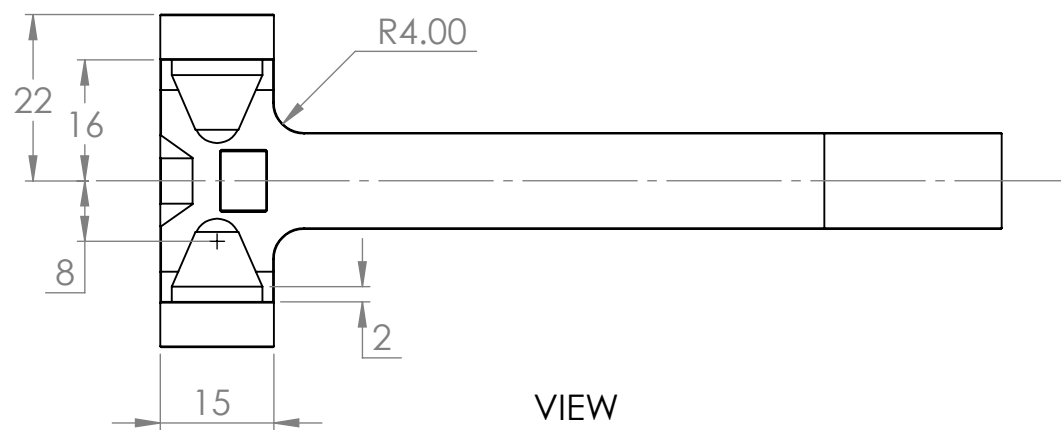
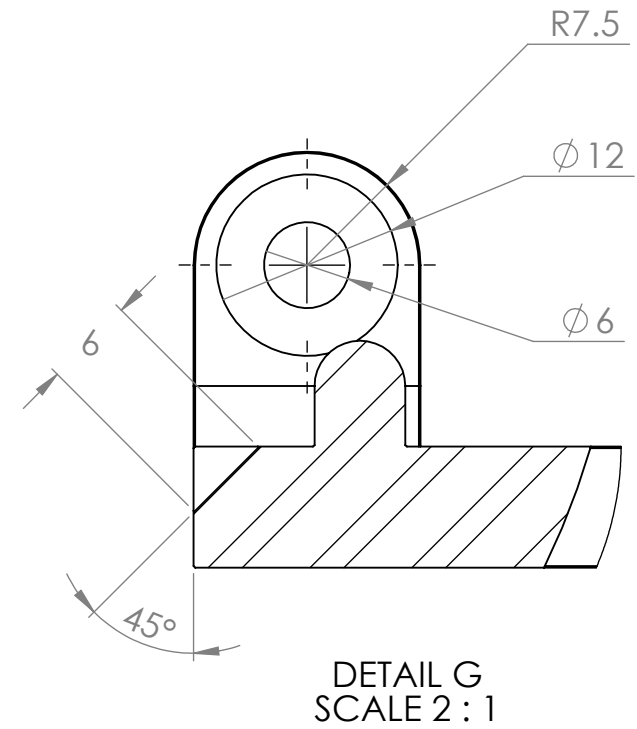
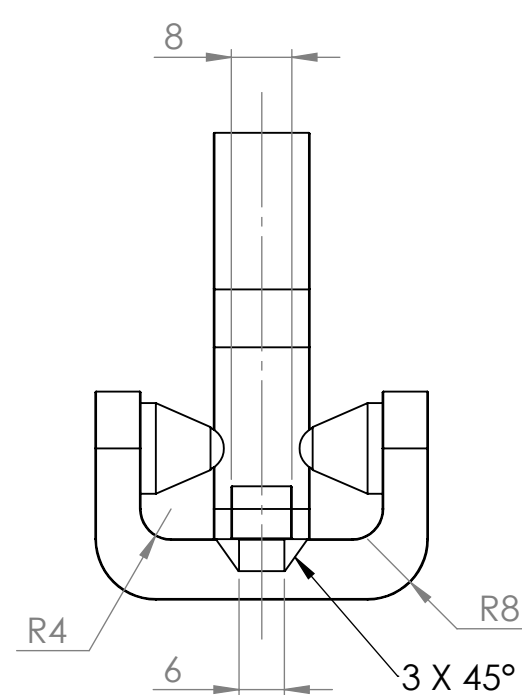
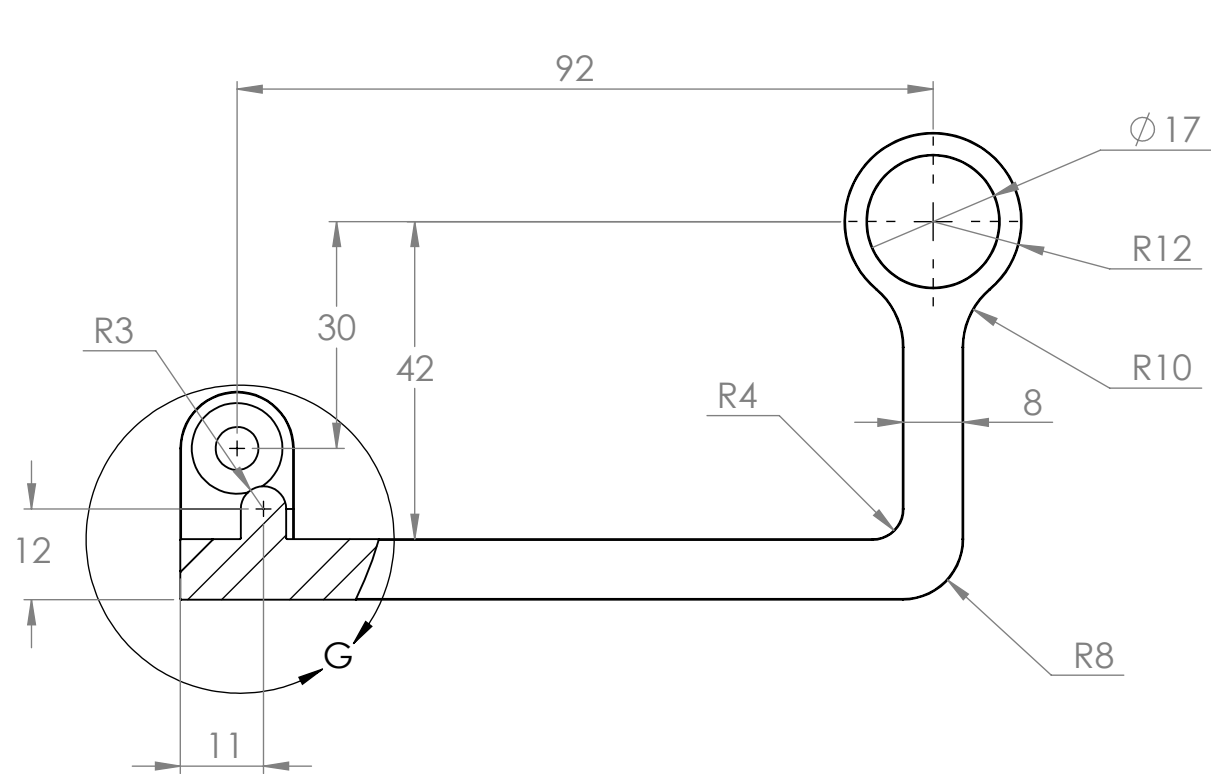


DO NOT SCALE DRAWING		FINISH:		REVISION:		TITLE:			
UNLESS OTHERWISE SPECIFIED: DIMENSIONS ARE IN MILLIMETERS SURFACE FINISH: TOLERANCES: LINEAR: ANGULAR:		DEBURR AND BREAK SHARP EDGES				3/8" Square Socket Extension			
	NAME	SIGNATURE	DATE	MATERIAL: AISI 321 Stainless Steel		PART NO.		39	A3
DRAWN									
CHK'D									
APPV'D				WEIGHT: 36.68		SCALE:3:1		SHEET 13 OF 17	

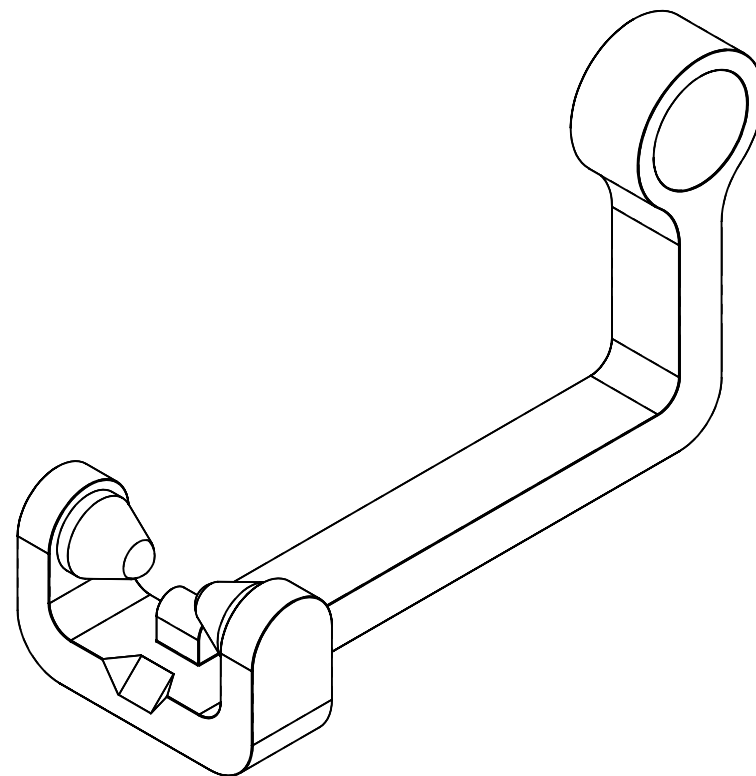




DO NOT SCALE DRAWING				FINISH:		REVISION:		TITLE:	
UNLESS OTHERWISE SPECIFIED: DIMENSIONS ARE IN MILLIMETERS SURFACE FINISH: TOLERANCES: LINEAR: ANGULAR:				DEBURR AND BREAK SHARP EDGES				Geneva Drive wheel	
	NAME	SIGNATURE	DATE	MATERIAL:		PART NO.		A3	
DRAWN				7075 Aluminium		6			
CHK'D									
APPV'D				WEIGHT: 12.46		SCALE:3:1		SHEET 16 OF 17	



VIEW



ISOMETRIC VIEW

DO NOT SCALE DRAWING				FINISH: DEBURR AND BREAK SHARP EDGES		REVISION: 		TITLE: <h1>Swing Arm</h1>	
UNLESS OTHERWISE SPECIFIED: DIMENSIONS ARE IN MILLIMETERS SURFACE FINISH: TOLERANCES: LINEAR: ANGULAR:				MATERIAL: Swing Arm		PART NO. 7		A3	
DRAWN		SIGNATURE	DATE	WEIGHT: 188.89		SCALE: 1:1		SHEET 17 OF 17	
CHK'D									
APPV'D									

APPENDIX B

Table 1: FEA stress, strain, and displacement data for key components of the model [15, 16]

Component Description	Min Stress (N/m ²)	Max Stress (N/m ²)	Min Yield Strength (N/m ²)	Max Displacement (mm)	Min Strain	Max Strain
Tool Arm	3.17e+01	2.12e+06	3.00e+07	2.10e-02	6.05E-10	2.41E-05
Swing Arm	6.96e+01	2.75e+07	2.50e+08	1.47e-01	5.34E-10	9.79E-05
Attachment	5.68e+01	3.71e+05	3.00e+07	4.13e-05	2.96E-09	3.35E-06
Link	2.10e+00	1.06e+07	2.50e+08	3.08e-03	2.45E-11	3.10E-05
Sprocket	7.00e+03	1.16e+07	3.00e+07	1.47e-02	1.01E-07	1.12E-04